Critical Reviews in Surface Chemistry, 4(3/4):141–187 (1994)

Supported Vanadium Oxide Catalysts: Molecular Structural Characterization and Reactivity Properties

Goutam Deo and Israel E. Wachs

Zettlemoyer Center for Surface Studies, Department of Chemical Engineering, Lehigh University, Bethlehem, PA 18015

Jerzy Haber

Institute of Catalysis and Surface Chemistry, Polish Academy of Science, 30-239 Krakow, Poland

ABSTRACT: Supported vanadium oxide catalysts have become an important class of catalytic materials because of their numerous industrial applications and use as model systems for fundamental studies of monolayer catalysts. This critical review of supported vanadium oxide catalysts examines our current understanding of the molecular structures of the two-dimensional vanadium oxide overlayers and their reactivity properties. The insights obtained from these structural and reactivity studies are establishing a fundamental understanding of supported vanadium oxide catalysts and allowing the development of structure-reactivity relationships. The findings for supported vanadium oxide catalysts are also directly applicable to other supported metal oxide systems, especially those that possess surface redox sites (Mo, Cr, and Re).

KEY WORDS: Metal oxide systems, molecular structural characterization, reactivity properties, vanadium oxide catalysts, surface redox sites.

1. INTRODUCTION

A number of researchers in the 1970s believed that the two-dimensional metal oxide overlayers that formed on oxide supports were unstable and that the metal oxide overlayers needed an extended three-dimensional (bulk) structure to be effective catalysts.[1] The concept of metal oxide monolayers lay in the realization that unique surface metal oxide species were present and stable on the surface of oxide supports. This controversial metal oxide monolayer proposal, that there existed a surface metal oxide phase different from bulk metal oxide phases, led most of the initial characterization studies to determine the existence and stability of these two-dimensional metal oxide overlayers. Supported vanadium oxide catalysts are an integral part of this larger family of supported metal oxide catalysts and became the model system because of wide use in industrial applications as oxidation catalysts. The presence of a stable surface vanadium oxide phase or monolayer, different from the bulk V_2O_5 phase, was established using various characterization techniques (e.g., XPS, Raman, IR, EXAFS/XANES), and the

1049-9407/94/$5.00

initial concerns about the vanadium oxide monolayers on a number of oxide supports were not found to be valid.[1]

Supported vanadium oxide catalysts find a variety of applications in a number of heterogeneous catalytic oxidation reactions.[1-7] In these catalysts, the vanadium oxide phase on the surface of an oxide support (e.g., TiO_2) is the active phase and is usually more active than bulk crystalline vanadium pentoxide (V_2O_5).[1] These observations stimulated detailed investigations of the nature of the surface vanadium oxide phase in an effort to determine the factors that control the formation and reactivity of an effective supported vanadium oxide catalyst. Information about the nature of the surface vanadium oxide phase was derived from physical and chemical characterization techniques. The physical characterization techniques provide insight into the structure of the surface vanadium oxide phase, and the chemical characterization techniques provide insight into the reactivity of the surface vanadium oxide phase. Correlating the structure and the reactivity properties of the surface vanadium oxide phase is of paramount importance in gaining a fundamental understanding into the origin of the unique properties provided by supported vanadium oxide catalysts.

This article on supported vanadium oxide catalysts is a critical review of our current understanding of the molecular structure and reactivity relationships of this important class of catalytic materials (for a detailed literature review, see refs. 1 and 2). To better understand the structural aspects of the supported vanadium oxide catalysts, the aqueous and solid state structural chemistry of vanadium oxide as well as different characterizations methods typically used to obtain such structural information are initially discussed. The discussion on the different characterization techniques emphasizes the type of molecular structural information as well as the limitations of the different spectroscopic techniques. Application of these modern spectroscopic methods is currently providing the critical molecular structural information of supported vanadium oxide catalysts. The reactivity of supported vanadium oxide catalysts is discussed for numerous oxidation reactions. Comparison of the molecular structure and reactivity information is beginning to establish a fundamental molecular understanding of this important class of catalytic materials.

II. VANADIUM OXIDE STRUCTURAL CHEMISTRY

Vanadium has the electron configuration $3d^3\ 4s^2$ in addition to the completed inner electron shells. Vanadium(V) ,$3d^0$, oxide compounds exist in a number of different coordinations and structures. The radius ratio of the vanadium(V) atom to the oxygen atom is rather large to form four coordinated structures and rather small for forming six coordinated structures. Perhaps for this reason vanadium(V) oxide compounds are present in nature as four, five, or six coordinated species. To appreciate the different structural properties of vanadium(V) oxide, it is beneficial briefly to touch upon its aqueous and solid state chemistry.

A. Vanadium (V) Oxide Structures in Aqueous Media

The different possible coordinations of vanadium(V) oxide are demonstrated in the aqueous chemistry of the vanadium(V) ion in solutions of different pH and ionic strength. The vanadium(V) ion is the stable oxidation state in aqueous solutions in the presence of air and is described in some detail by Baes and Mesmer.[8] Twelve different vanadium(V) oxide species are known to exist in aqueous solutions. At high pH values (basic region) and low vanadium(V) ion concentrations, the vanadium(V) oxide species is four coordinated and isolated (VO_4^{3-}); at low pH values and high vanadium(V) ion concentrations, the vanadium(V) oxide species is present as polymerized and six coordinated decavanadates, $V_{10}O_{28-z}(OH)_z^{z-6}$. Intermediate values of pH and vanadium(V) ionic concentrations give rise to various levels of polymerization and protonation of four and six coordinated vanadium(V) oxide species (e.g., $V_2O_6(OH)^{3-}$, $V_3O_9^{3-}$, $V_{10}O_{27}(OH)^{5-}$).

B. Vanadium(V) Oxide Structures in the Solid State

Vanadium(V) oxide structures in solids are usually very distorted in comparison with the aqueous phase structures. However, certain examples exist in the solid state that bring out some of the regular coordinations of the vanadium(V) oxide structures. Vanadium(V) oxide structures can be generally categorized as four coordinated vanadates (orthovanadates, pyrovanadates, and metavanadates), five coordinated vanadates, and six coordinated vanadates.

Orthovanadates containing isolated VO_4 units include $Pb_5(VO_4)Cl$,[9] $BiVO_4$,[10] Na_3VO_4,[11] and α-$Zn_3(VO_4)_2$[12] and are the least distorted of the four coordinated vanadates. These orthovanadates are characterized by possessing nearly equal vanadium oxygen bond length ranging from 1.69 to 1.77Å. Pyrovanadates contain V_2O_7 dimeric units and are found in $Cd_2V_2O_7$,[13] α-$Zn_2V_2O_7$,[14] and α-$Mg_2V_2O_7$.[15] The presence of a V-O-V bridge results in a short vanadium oxygen terminal bond length, 1.658 to 1.672 Å. The α-$Mg_2V_2O_7$ structure is not an ideal pyrovanadate, but possesses a long fifth V-O bond (2.4 – 2.9 Å). Metavanadates possess polymeric chains of -(VO_2)-O-units and can be found in NH_4VO_3[16] and α-$NaVO_3$.[17] The two terminal vanadium oxygen bonds in the VO_2 units range from 1.63 to 1.67Å, and the vanadium oxygen distances in the V-O-V bridging bonds are 1.8 Å. In addition to the above four coordinated structures, unusual vanadium oxide structures can be found in $AlVO_4$ and $FeVO_4$ which possess highly distorted and isolated VO_4 units.[18]

Six coordinated vanadium oxide structures are found in PbV_2O_6,[19] V_2O_5,[20] and $Na_6V_{10}O_{28} \cdot 18H_2O$.[21] Two distinct types of VO_6 units can be found in PbV_2O_6. The structure of V_2O_5 contains chains of highly distorted VO_6 units with one short apical V-O bond at 1.58 Å, an opposing long V-O bond at 2.78 Å, and four bridging V-O bonds lying roughly in a plane at 1.78, 1.88 (×2), and 2.02 Å. The decavanadate unit in $Na_6V_{10}O_{28} \cdot 18H_2O$ contains essentially five different VO_6 units. Four of

these VO_6 units possess terminal vanadium oxygen bonds similar to V_2O_5 and each of the four terminal V=O bonds are distinct from each other. The fifth VO_6 unit does not, however, possess a terminal vanadium oxygen bond, and all of its oxygen atoms are part of V-O-V bridging bonds.

In the solid state, vanadium and oxygen form different types of vanadium oxides in addition to V_2O_5. In these vanadium oxides, vanadium possesses oxidation states lower than 5. A number of studies have dealt with the coordination and catalysis of vanadium oxides with interesting features regarding the stability, oxygen diffusion, and correlation of the vanadium oxide phases present under reaction environments.[22] Even though the structure and reactivity of the surface vanadium oxide species on supported vanadium oxide catalysts are different from the structure of bulk V_2O_5, it is helpful to keep in perspective the general trends in behavior of V_2O_5 and its suboxides (vanadium oxidation state less than +5) during different reaction environments.

III. CHARACTERIZATION TECHNIQUES FOR SUPPORTED VANADIUM OXIDE CATALYSTS

Surface vanadium oxide phases are formed when vanadium oxide is deposited on an oxide support (Al_2O_3, TiO_2, SiO_2, etc.). The supported vanadium oxide phase, like other supported metal oxide phases, can simultaneously exist in several different states (bulk crystallites, mixed phases with the support, or two-dimensional overlayers) that possess different structures. The presence of these multiple phases makes the analysis of the supported vanadium oxide phase extremely challenging. Recent developments in molecular characterization techniques have successfully demonstrated the capability to discriminate between the multiple vanadium oxide structures present in supported vanadium oxide catalysts and provide the information required to develop a molecular level understanding of these complex catalytic materials.

A. Raman Spectroscopy

Several studies have shown that Raman spectroscopy can readily discriminate between different vanadium oxide structures with different coordinations and bond lengths.[23–31] These studies also revealed that the vanadium-oxygen vibrations are present below 1,100 cm^{-1}. A recent development in the application of Raman spectroscopy for the study of vanadium oxide structures is the Raman frequency-vanadium oxygen bond length correlation.[31] Using this correlation, the bond length of a vanadium-oxygen bond can be determined from its corresponding Raman frequency. The simultaneous use of model vanadium oxide compounds and the Raman frequency-bond length correlation makes Raman spectroscopy ideally suited to study the amorphous structures of the surface vanadium oxide species

present on oxide supports because of the numerous possible vanadium oxide structures in such supported catalysts. This has been demonstrated in various Raman spectroscopy studies of supported vanadium oxide catalysts.[29–54] However, it has not always been possible completely to determine all the structures of the surface vanadium oxide species strictly from Raman spectroscopy because not all vibrational modes are Raman active (especially bonds to the oxide supports), and sometimes there is an overlap of the support vibrations especially in the lower frequency region (<700 cm^{-1}).

Raman spectroscopy is an optical technique and, therefore, can be applied to study the structural changes of the surface vanadium oxide species under *in situ* conditions where the environment around the catalyst is controlled (temperature, pressure and gas composition). Even though Raman spectroscopy is a bulk technique, it provides information about the surface vanadium oxide species since they are located on the oxide support surface.[55] The limitations of Raman spectroscopy for the characterization of supported vanadium oxide catalysts occur when the vibrations of the oxide support overlap the vibrations arising from the surface vanadium oxide phase. In such a situation it is necessary to take advantage of other structural characterization techniques (e.g., solid state ^{51}V NMR). The theory and application of Raman spectroscopy to catalytic material can be found elsewhere.[56]

B. Infrared Spectroscopy

Infrared (IR) spectroscopy is a bulk technique that also takes advantage of the surface aspect of the supported vanadium oxide phases. Infrared spectroscopy can also discriminate between various vanadium oxide structures. [57] However, many of the oxide supports obscure the vibrations arising from the supported vanadium oxide phase because they absorb the infrared signal (especially below 1,000 cm^{-1}).[58] For some systems it is at least possible to obtain the highest frequency of the surface vanadium oxide species, which usually corresponds to the vanadium oxygen terminal bonds.[34,42,46,48,54,58–60] IR spectroscopy, however, provides additional information about the surface vanadium oxide species, which complements the vibrations observed by Raman spectroscopy and also can be used under *in situ* conditions. IR spectroscopy is more frequently used in probing reactant molecules in the course of adsorption and surface reaction rather than the surface vanadium oxide phase due to the problems associated with observing vanadium oxygen vibrations occurring less than 1,000 cm^{-1} (e.g., oxidation of methanol,[61–63] oxidation of propylene,[64] ethylene,[65] n-butenes and isobutene,[66] and oxidation of methyl aromatics.)[67] Adsorption of basic molecules (e.g., ammonia, pyridine) provides information about the distribution of surface Lewis and Bronsted acid sites.[48,60,68–70] IR also provides direct information about the interaction of vanadium oxide with the surface hydroxyls of oxide supports.[70] Additional details about the theory and application of IR spectroscopy to catalytic materials can be found elsewhere.[71,72]

C. Solid-State ^{51}V Nuclear Magnetic Resonance Spectroscopy

The ^{51}V nucleus possesses excellent characteristics for NMR experiments due to its natural abundance (99.78%). These advantageous characteristics have resulted in a number of recent studies using solid-state ^{51}V nuclear magnetic resonance (NMR) spectroscopy for the characterization of supported vanadium oxide catalysts.[40,73–77] Solid-state ^{51}V NMR provides information about the oxygen coordination (four or six) as well as structural information about the supported vanadium oxide phase. Solid-state ^{51}V NMR, similar to Raman and IR spectroscopy, is also a bulk technique that takes advantage of the surface location of the supported vanadium oxide phase to provide surface information. In addition to providing coordination and structural information about the surface vanadium oxide phase, solid-state ^{51}V NMR is quantitative and reveals the distribution of different vanadium oxide phases simultaneously present. The limitation of solid-state ^{51}V NMR is that vanadium in the +4 oxidation state broadens the NMR signal, and consequently, the signal due to the vanadium(V) nucleus can be lost. Fortunately, vanadium(IV) oxide is present in very small amounts in calcined catalysts.[78] However, the concentration of vanadium (IV) oxide under reaction conditions may vary over a wide range[79,80] and ^{51}V NMR may not be compatible with *in situ* studies. An additional limitation of solid state NMR is the somewhat lower sensitivity compared to vibrational techniques.[72] Information about the theory and application of solid state ^{51}V NMR to supported vanadium oxide catalysts can be found elsewhere.[72,74]

D. X-Ray Absorption Spectroscopy

X-ray absorption spectroscopy takes advantage of intense synchrotron X-ray sources to determine the oxidation state and chemical environment around a specific element in the sample. Similar to the above spectroscopies, it is a bulk technique but provides surface information for the highly dispersed supported vanadium oxide phase. X-ray absorption spectroscopy is an ideal tool to examine the chemical environment around vanadium in supported vanadium oxide catalysts because the fine structure associated with the vanadium edge is specifically associated with the immediate chemical environment of the vanadium atom. The oxygen coordination and vanadium-oxygen bond lengths can be calculated from the different mathematical treatments of the X-ray fine structure. X-ray absorption techniques (EXAFS/XANES) have been used to determine the molecular structures of the surface vanadium oxide phase with some success.[81–85] Furthermore, X-ray absorption spectroscopy can be used under *in situ* conditions. The disadvantage of the X-ray absorption techniques is that only an average signal of the different vanadium oxide structures is observed and hence, only the average structure can be obtained. Thus X-ray absorption spectroscopy can be used effectively to provide fundamental structural information of the surface vanadium oxide species

only if one species is present that must be confirmed by other spectroscopies (e.g., Raman or ^{51}V NMR).

E. X-Ray Photoelectron Spectroscopy

X-ray photoelectron spectroscopy (XPS) provides information about the oxidation state and dispersion in the surface region (2 – 20 atomic layers) of the catalyst.[72] The most common method used to determine the dispersion of the surface vanadium oxide species is by measuring the XPS vanadium to the support cation intensity ratio (I_v/I_s, S= Support Cation). Below monolayer coverages, the I_v/I_s intensity ratio increases linearly with vanadium oxide coverage and then reaches a relatively constant value above monolayer vanadium oxide coverages.[86] Models have been proposed to determine the surface atomic ratios from the intensity ratio, I_v/I_s.[87] However, molecular structural information of the surface vanadium oxide phase cannot be obtained using XPS since it cannot discriminate between different vanadium oxide structures possessing the same oxidation state. Furthermore, XPS requires high vacuum conditions for its operation and cannot be used under *in situ* conditions. XPS is especially useful when reduced vanadium oxide states are present.

F. Electron Paramagnetic Resonance Spectroscopy

Electron paramagnetic resonance (EPR) is also a bulk characterization technique that is effective in determining the nature of paramagnetic species such as vanadium in the +4 oxidation state immersed in diamagnetic matrices. This is possible since the *g* factor and hyperfine splitting, arising from an interaction of the unpaired electron with the ^{51}V nucleus, are extremely sensitive to the chemical environment around the paramagnetic V^{+4} ion.[88] This extreme sensitivity had led to much confusion in the literature because many EPR studies have focused on trace amounts of vanadium(IV) oxide species in catalysts rather than the most abundant species. This is especially true for calcined supported vanadium oxide catalysts where vanadium is almost exclusively present as vanadium(V) oxide. Thus it is critical that such studies quantify the fraction of vanadium atoms being monitored by EPR. Furthermore, EPR studies are usually not amenable to *in situ* studies under reaction environments due to signal broadening at elevated temperatures.[89] An additional limitation of the EPR technique is that it is ideally applicable for isolated V^{4+} ions due to the problems associated with signal broadening and spin-spin coupling for paired V^{4+} ions. Consequently, reported EPR studies always should be carefully examined for their experimental methodology and conclusions. In spite of the above potential complications, EPR is one of the few characterization techniques than can provide molecular structural information about reduced vanadium (IV) oxide species.[90–93]

G. Ultraviolet Visible (UV-VIS) Spectroscopy

Ultraviolet and visible spectroscopy takes advantage of the different electronic transitions of metal ions that depend on the symmetry and environment. The application of ultraviolet and visible (UV-vis) spectroscopy for the study of supported vanadium oxide catalysts has also received some attention.[54,94–96] However, the origin of the specific electronic transition is sometimes difficult to isolate since the electronic transition depends on various parameters. For supported molybdenum oxide systems, the increasing signficance of these parameters were classified as:

local symmetry < overall symmetry < condensation degree, polarization effect and size of the countercation, and dispersion on a support.[97,98] Similar effects also may be present for supported vanadium oxide catalysts. The broad UV-vis bands also decrease the sensitivity for certain species. However, UV-vis spectroscopy can be successfully applied to supported vanadium oxide catalysts in conjunction with other characterization techniques (e.g., Raman and NMR). Studies utilizing such a complementary characterization approach are currently underway.[99]

H. Temperature Programmed Reduction

Numerous experiments using temperature programmed reduction for the characterization of supported vanadium oxide catalysts have been performed because these catalysts form an important class of oxidation catalysts that usually undergo reduction during the catalytic cycle. A measure of the reduction characteristics is provided by TPR experiments.[100] The TPR experiments can potentially discriminate between different metal oxide phases provided the reducibilities are significantly different. This has been shown for the reducibility of different supported and unsupported vanadium oxide catalysts.[101,102] However, most of the TPR studies reported do not appear as sensitive as vibrational spectroscopies or solid-state ^{51}V NMR because only one peak is typically observed in the reported TPR profiles when the physical characterization studies show the presence of some bulk V_2O_5 as well as more than one molecularly dispersed species. One TPR peak is in fact observed for four monolayers of vanadium oxide supported on TiO_2.[103] In spite of this limitation, the TPR experiments have been successfully applied to studying supported vanadium oxide catalysts,[101,102] which have revealed that the TPR profile of the surface vanadium oxide phase depends on the nature of the specific oxide support. More recent high-resolution TPR experiments readily discriminate between surface vanadium oxide and crystalline V_2O_5 phase and provide for the quantitative determination of surface vanadium oxide species.[104] The TPR experiments, however, do not provide structural information about the surface vanadium oxide phase and are limited to environments containing hydrogen or other reducing gases.

I. Chemisorption Techniques

Chemisorption of gases have been used to study the monolayer coverage limits as well as dispersion of supported vanadium oxide catalysts, but cannot provide molecular structural information. A number of studies elaborate on the use of low temperature oxygen chemisorption (LTOC) to study the amount of oxygen chemisorbed after reducing the supported vanadium oxide catalysts.[105–110] These studies reveal that the moles of oxygen chemisorbed at low temperature on the reduced supported vanadium oxide catalysts increase up to monolayer coverages and decrease for loadings greater than monolayer coverages. The conclusions obtained by the LTOC method are indirect, and no structural information can be obtained regarding the surface vanadium oxide phase. The application of the LTOC technique has recently been disputed due to the overreduction of vanadium oxide and the underestimation of the oxygen adsorption capacity.[45] Uncertainty of the extent of reduction of the vanadium oxide phase always complicates oxygen chemisorption methods.

Chemisorption of carbon dioxide and benzaldehyde-ammonia titration (BAT) probe the exposed oxide support of the supported vanadium oxide catalysts by interacting with the basic surface hydroxyls.[111,112] These chemisorption techniques are not applicable to the rather neutral SiO_2 surface. These chemisorption probes can usually determine monolayer coverages since no chemisorption occurs since the majority of the surface hydroxyls are removed at monolayer coverage. However, they may not always be quantitative at intermediate surface coverages of surface vanadium oxide species since they selectively interact with basic surface hydroxyls, which may not always be representative of the entire exposed surface.[113] Thus these chemisorption techniques can give good estimates of monolayer coverages of the surface vanadium oxide overlayers on oxide supports.

The nitric oxide-ammonia rectangular pulse (NARP) method was also applied to determine the surface coverage of the vanadium oxide overlayer.[114,115] This method was initially developed for bulk V_2O_5 and extended to supported vanadium oxide catalysts by assuming that the surface vanadium oxide species possesses similar structures and properties as bulk V_2O_5 (exposed (010) crystal face). However, more recent studies reveal that both the structure and reactivity of the surface vanadium oxide overlayer are not related to that of bulk V_2O_5, but are dramatically influenced by the vanadium oxide coverage and specific oxide support (see parts IV and V on molecular structures and reactivity). Thus the current findings suggest that the NARP techniques are probing the reactivity of the surface vanadium oxide overlayers on oxide supports for the NO/NH_3 reaction rather than providing quantitative information about the surface vanadium oxide coverage or special exposed vanadium oxide sites.

J. Chemical Analysis

The method is based on selective extraction followed by dissolution and chemical analysis.[93,116,117] Using dilute H_2SO_4 or ammonia solution, the soluble

portion of the vanadia species present at the surface may be extracted and quantitatively determined. They are considered as vanadia species weakly interacting with the surface. The residual sample is dissolved in boiling concentrated H_2SO_4 and the amount of vanadium is determined by a titration method. This part constitutes the vanadia species strongly interacting with the surface. Attempts also have been made to determine by chemical methods the valence state of strongly and weakly bonded vanadium ions. It has been claimed[79,80] that strongly bonded vanadium oxide species on anatase and rutile surface contain four valent vanadium ions. This result has been, however, questioned due to the redox processes occuring in the course of dissolution and chemical analysis.[118]

K. Summary

In summary, the physical characterization techniques (e.g., Raman, NMR, IR) are essentially bulk techniques that take advantage of the surface nature of the supported vanadium oxide phase. Of these techniques, Raman and solid-state ^{51}V NMR spectroscopy are best suited for molecular characterization of vanadium(V) oxide. X-ray absorption and IR spectroscopies are good complementary techniques when used in conjunction with Raman and NMR. XPS can be used only to study the oxidation state and dispersion of the supported vanadium oxide phase. EPR and X-ray absorption can provide structural information about vanadium(IV) species. Chemisorption techniques provide indirect information about the dispersion of the surface vanadium oxide phase and usually require the assumption of certain stoichiometries. Temperature programmed reduction studies are best suited for studying the dispersion and reduction behavior of the surface metal oxide species. UV-Vis, however, is not a very informative characterization technique for supported vanadium oxide catalysts when applied independently. Chemical analysis of vanadium oxide species by dissolution and titration is questionable. Characterization techniques most suitable for *in situ* reaction studies are Raman, IR, X-ray absorption (EXAFS/XANES), and to a limited extent EPR and UV-vis.

IV. MOLECULAR STRUCTURES OF SUPPORTED VANADIUM OXIDE CATALYSTS

Knowledge of the structure of the surface vanadium oxide species in supported vanadium oxide catalysts is critical to the fundamental understanding of the surface vanadium oxide phase-support and surface vanadium oxide phase-reactant gas interactions. The structure of the surface vanadium oxide phase in supported vanadium oxide catalysts depends on both the particular gas and solid environment. Recent developments in the characterization of surface vanadium oxide

phases with the use of one or more of the characterization techniques mentioned in the previous section have had a major impact on determining the molecular structure of the surface vanadium oxide species. The structure of the surface vanadium oxide species in supported vanadium oxide catalysts is discussed here with respect to the different environments experienced.

A. Surface Vanadium Oxide Structures Under Ambient Conditions

Many previous structural characterization studies of the surface vanadium oxide species on oxide supports were obtained under ambient conditions where a significant amount of moisture is present (see below). It was observed that the structure of the surface vanadium oxide species under ambient conditions was a function of various factors,[33,38,39,41,44,119–122] which can be categorized as specific oxide support, vanadium oxide loading, preparation method, calcination temperature, and impurities/promoters. The potential contributions of all these factors make it difficult to make a conclusive determination of the individual contributions of these factors upon the structure of the surface vanadium oxide species under ambient conditions from the published literature. Thus to elucidate the nature of the surface vanadium oxide species on different oxide supports, under ambient conditions, various loadings of vanadium oxide catalysts (monolayer and submonolayer) were systematically prepared on different oxide supports that are listed in Table 1. Most of the vanadium oxide overlayers were prepared by the incipient wetness impregnation of vanadium triisopropoxide oxide and methanol solutions in a controlled environment (flowing N_2). After impregnation and thorough mixing, the oxide support and alkoxide solution were dried in the glove box for 16 hours and subsequently heated to 120°C in flowing nitrogen. The final calcination was performed in O_2 at 450°C for vanadium oxide supported on ZrO_2, Nb_2O_5, and TiO_2 and at 500°C for vanadium oxide supported on Al_2O_3 and SiO_2. The ZrO_2, Nb_2O_5, and TiO_2 supported vanadium oxide catalysts were calcined at slightly lower

TABLE 1
Support Specifications[a]

Support	Supplier	Surface area (m^2/g)
MgO	Fluka	80
γ-Al_2O_3	Harshaw	180
TiO_2	Degussa	55
ZrO_2	Degussa	39
Nb_2O_5	Niobium Products	55
SiO_2	Cabot	300

[a] Pretreatment temperature of supports can be found in refs. 49, 123.

temperatures in order to assure that sintering of these less thermally stable oxide supports did not occur.

The maximum amount of dispersed vanadium oxide that could be obtained on the different oxide supports was 11–15 μmole V^{5+}/m^2, with the exception of SiO_2 and MgO supports.[123] On SiO_2, the maximum amount of vanadium oxide that can be dispersed corresponds to 1 μmole V^{5+}/m^2 because of the weak interaction of metal oxides with the silica surface. The maximum amount of vanadium oxide that could be dispersed on MgO was not determined due to complications of compound formation between vanadium oxide and MgO (see the following section on dehydrated surface vanadium oxide structures).

Structural information about the surface vanadium oxide species under ambient conditions was obtained using Raman spectroscopy and solid-state ^{51}V NMR spectroscopy and are tabulated in Table 2 as a function of vanadium oxide coverage and oxide support. An example of this structural characterization is exemplified by the 10% V_2O_5/γ-Al_2O_3 sample, where a complete match of the Raman spectra of the 10% V_2O_5/γ-Al_2O_3 under ambient conditions and the decavanadate ion in $Na_6V_{10}O_{28} \cdot 18H_2O$ were obtained indicating the same molecular structures.[49] Similar solid-state ^{51}V NMR powder spectra were also observed for the 10% V_2O_5/γ-Al_2O_3 sample and $Na_6V_{10}O_{28} \cdot 18H_2O$.[74]

Examination of Table 2 reveals two important trends. Upon increasing the vanadium oxide loading to monolayer coverage, the surface vanadium oxide structures become more polymerized and in most cases (except V_2O_5/MgO) are primarily six coordinated at monolayer coverages. Polymerization is defined here as the repetition of the basic four or six coordinated unit with the formation of V-O-V linkages. Furthermore, if the supports are arranged in the order shown in Table 2, more polymerized and six coordinated surface vanadium oxide structures are formed as one goes down the series. Thus, the surface vanadium oxide structure depends on the oxide support and the vanadium oxide surface coverage.

TABLE 2
Surface Vanadium Oxide Species on Different Oxide Supports under Ambient Conditions

Oxide support	Low coverage	High coverage
MgO	VO_4,[a] V_2O_7, $(VO_3)_n$	VO_4,[a] V_2O_7,[a] $(VO_3)_n$
γ-Al_2O_3	$(VO_3)_n$[a]	$(VO_3)_n$, $V_{10}O_{28}$[a]
TiO_2	$(VO_3)_n$,[a] $V_{10}O_{28}$	$V_{10}O_{28}$[a]
ZrO_2	V_2O_7, $(VO_3)_n$,[a] $V_{10}O_{28}$	$V_{10}O_{28}$[a]
Nb_2O_5	$(VO_3)_n$[a]	$V_{10}O_{28}$[a]
SiO_2	$V_2O_5 \cdot nH_2O$[a]	bulk V_2O_5[a]

[a] Major species.

As described earlier in part II, the type of vanadium oxide species present in aqueous solutions is a function of the amount (ionic concentration) of vanadium oxide present and the pH of the solution.[8] For small amounts of vanadium oxide species and high pH values, the vanadium oxide species in aqueous solution are four coordinated and isolated, whereas for high vanadium oxide amounts and low pH values, more polymeric and six coordinated vanadium oxide species (decavanadate) are present. For intermediate pH values and vanadium oxide amounts, the vanadium oxide species in aqueous solution is present as a combination of four and six coordinated species in various degrees of polymerization. The similarity between the molecular structures of the surface vanadium oxide species under ambient conditions with the vanadium oxide species in aqueous solutions suggests a common underlying factor controlling the molecular structures of the vanadium species.

Analysis of the various supported vanadium oxide catalysts (pure oxide support and supported vanadium oxide samples) show that under ambient conditions moisture is present on the surface of all of these samples. The presence of surface moisture is shown from TGA experiments, which reveal that oxide supports desorb water as they are heated.[74] The weight loss (%) due to the desorption of surface moisture on the various oxide supports due to heating to 400°C are shown in Table 3. Similar amounts of water per surface area are present on the different oxide supports with the exception of SiO_2, which exhibits a much lower water content due to its hydrophobic nature. The amount of water present on the different oxide supports is in excess of 20 monolayers, and consequently, it is not surprising that proton NMR of the supported vanadium oxide samples indicate that the surface moisture under ambient conditions is similar to water.[74]

Oxide supports in the presence of water impart a specific pH at the surface, which is measured as the surface pH at point of zero charge (pzc) from electrophoretic measurements. The formation of a specific pH at pzc at the surface of the oxide support is proposed to occur through proton exchange.[124] Analysis of the

TABLE 3
Weight Loss of Oxide Supports Upon Heating in Air to 500°C

Oxide support	Surface area (m^2/g)	Weight loss (%)/m^2
MgO	80	ND
γ-Al_2O_3	180	0.042
TiO_2	55	0.028
ZrO_2	39	0.038
Nb_2O_5	55	0.036
SiO_2	300	0.004

ND = not determined.

surface pH at pzc of the various oxide supports, shown in Table 4, reveals that the surface pH at pzc decreases as one goes down the series: MgO has the highest surface pH at pzc and SiO_2 has the lowest surface pH at pzc. Hence, the moisture on the surface of the different oxide supports possesses a certain pH that is specific for the particular oxide support. The presence of moisture on the surface of the various oxide supports establishes that the surface vanadium oxide species is essentially in an aqueous solution. At low vanadium oxide loadings, the surface vanadium oxide species under ambient conditions is in solution in the surface moisture layers at a pH that is essentially controlled by the specific oxide support. If the surface pH were to control the molecular structure of the surface vanadium oxide species under ambient conditions, analogous to the aqueous phase diagram,[8] the surface vanadium oxide species would be expected to become more polymerized and be predominantly six coordinated as one goes down the series of oxide supports presented in Table 5. Examination of Table 5 shows that this is indeed the case since a close correspondence exists between the predicted and observed surface vanadium oxide species. The MgO support that has a pH at pzc of ~11 possesses essentially isolated four coordinated units and the SiO_2 support that has a pH at pzc of ~4 possesses predominantly six coordinated species.

In addition to the oxide support imparting a specific pH on the surface moisture layer, bulk vanadium oxide also imparts a low surface pH at pzc[125]. Potentiometric titration shows[126] that the dependence of pzc for a system of metal oxide supported on another metal oxide, e.g., vanadium oxide/anatase, on the surface coverage is not linear and the strongest effect is observed for low coverages. The value of pzc is shifted from pH = 6 to 6.4, characteristic of pure anatase, to about pH=4 at 25% coverage and to pH=3.4 for complete covered surface. From the aqueous phase diagram,[8] the decrease in pH values for the surface moisture layer would suggest more polymerized and six coordinated surface vanadium oxide species. This is confirmed in Table 6 since a close correspondence exists between the observed and predicted surface vanadium oxide species that are present on the various oxide supports under ambient conditions.

The close correspondence in predicted and observed vanadium oxide structures in Tables 5 and 6 indicates that the *net* surface pH at pzc of the surface

TABLE 4
pH at Point of Zero Charge (PZC) of the Oxide Supports

Oxide support	pH at PZC of oxide support
MgO	11
γ-Al_2O_3	8.9
TiO_2	6.0–6.4
ZrO_2	5.9–6.1
Nb_2O_5	4.3
SiO_2	3.9

TABLE 5
Predicted and Observed Vanadium Oxide Species on Different Oxide Supports: Low Vanadium Oxide Loadings

Oxide support	pH of support	Predicted low coverages	Observed low coverages
MgO	11	$VO_3(OH)$	VO_4,[a] V_2O_7, $(VO_3)_n$
γ-Al_2O_3	8.9	$VO_3(OH)$, V_2O_7	$(VO_3)_n$[a]
TiO_2	6.0–6.4	$VO_2(OH)_2$, $(VO_3)_n$	$(VO_3)_n$,[a] $V_{10}O_{28}$[a]
ZrO_2	5.9–6.1	$VO_2(OH)_2$, $(VO_3)_n$	V_2O_7, $(VO_3)_n$,[a] $V_{10}O_{28}$[a]
Nb_2O_5	4.3	$V_{10}O_{27}(OH)$, $(VO_3)_n$	$(VO_3)_n$[a]
SiO_2	3.9	V_2O_5, $V_{10}O_{26}(OH)_2$, $VO(OH)_3$	$V_2O_5 \cdot nH_2O$

[a] Major species.

moisture depends on the specific oxide support and the vanadium oxide loading and controls the structure of the hydrated surface vanadium oxide species. Thus the structure of the surface vanadium oxide species under ambient conditions is controlled by the *net surface pH at pzc* of the surface moisture layer, (illustrated in Figure 1). In Figure 1, the surface vanadium oxide species (hydrated surface VO_x) are shown to be present in the thin moisture layer on the surface of the oxide support (shown as the dashed box on top of the oxide support). This surface moisture layer possesses a certain net pH that is controlled by the oxide support and the surface vanadium oxide phase. The pH of the surface moisture layer, consequently, determines the structure of the surface vanadium oxide species. More recent studies are aimed at determining the exact pH value of the surface moisture layer, and such measurements confirm the above model.[127,128]

The model of the net surface pH at pzc of the surface moisture layer also explains the effect of calcination temperature, preparation method, and impurities/

TABLE 6
Predicted and Observed Vanadium Oxide Species on Different Oxide Supports: High Vanadium Oxide Loadings

Oxide support	pH of support	Predicted high coverages	Observed high coverages
MgO	11	$VO_3(OH)$, V_2O_7, $(VO_3)_n$	VO_4,[a] V_2O_7,[a] $(VO_3)_n$
γ-Al_2O_3	8.9	V_2O_7, $(VO_3)_n$	$(VO_3)_n$, $V_{10}O_{28}$[a]
ZrO_2	5.9–6.1	$(VO_3)_n$, $V_{10}O_{27}(OH)$	$V_{10}O_{28}$[a]
TiO_2	6.0–6.4	$(VO_3)_n$, $V_{10}O_{28}$	$V_{10}O_{28}$[a]
Nb_2O_5	4.3	$V_{10}O_{27}(OH)$	$V_{10}O_{28}$[a]
SiO_2	3.9	$V_{10}O_{26}(OH)_2$, V_2O_5	V_2O_5[a]

[a] Major species.

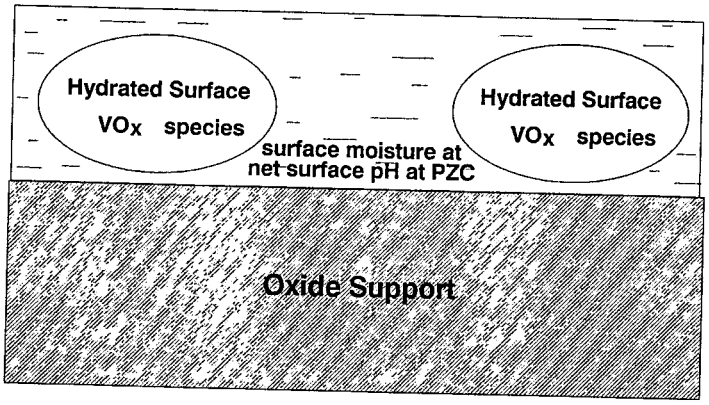

FIGURE 1. pH at PZC model for the surface vanadium oxide phase under ambient conditions. The surface vanadium oxide phase is shown as a hydrated species in a thin surface moisture layer.

promoters.[49] Higher calcination temperatures result in a decrease of the surface area of the oxide support, which increases the effective vanadium oxide loading per unit surface area and consequently, decreases the net surface pH at pzc. Based on the aqueous phase diagram of vanadium oxide,[8] the surface vanadium oxide structure under ambient conditions would be expected to be more polymerized and six coordinated at lower net surface pH at pzc. This effect is observed in the Raman spectra of 1% V_2O_5/TiO_2 where the Raman band shifts from ~950 cm^{-1} to ~970 cm^{-1} as the calcination temperature is increased from 450°C to 800°C and is indicative of the transformation of four and six coordinated surface vanadium oxide species present at 450°C to primarily six coordinated surface vanadium oxide species at 800°C. For constant vanadium oxide loading, the preparation method cannot change the surface pH as long as the precursor ligands are removed and the oxide support surface is not altered (e.g., sintering) during preparation because the preparation method does not affect the surface coverage of vanadium oxide.[49] Impurities and promoters affect the net surface pH at pzc of the surface moisture layer depending on their specific surface pH properties. For example, potassium oxide, which possesses a high surface pH, increases the surface pH at pzc and results in more isolated four coordinated species; tungsten oxide, which possesses a low surface pH, decreases the net surface pH at pzc and results in more polymerized and six coordinated surface vanadium oxide species.[49]

B. Surface Vanadium Oxide Structures under Dehydrated Conditions

Under typical reaction conditions involving supported vanadium oxide catalysts (300–700°C), desorption of the surface moisture present under ambient

conditions readily occurs as is evident from thermogravimetry and proton NMR experiments of the dehydrated samples.[74] Consequently, the structure of the surface vanadium oxide species on the different oxide supports under dehydrated conditions is no longer controlled by the net surface pH at pzc since an aqueous layer no longer exists on the surface at elevated temperature.

Under ambient conditions, the surface vanadium oxide species is in an aqueous solution in the surface moisture layer without being directly bonded to the support, and under dehydrated conditions, the surface vanadium oxide species directly bonds to the surface of the oxide support. The bonding of the surface vanadium oxide species to the surface of the oxide support is reflected in the gradual disappearance of the support surface hydroxyls with increasing vanadium oxide loading. The titration of the surface hydroxyls (OH) by the surface vanadium oxide species is directly monitored by *in situ* IR[70] and proton NMR[129] studies, which reveal the sequential disappearance of the OH bands. The consumption of the surface hydroxyls is also indirectly observed by CO_2 chemisorption studies since CO_2 forms carbonates with the surface hydroxyls.[130,131]

The desorption of the surface moisture layer present under ambient conditions from the vanadium oxide supported on titania catalyst results in a dramatic change in the Raman and solid-state ^{51}V NMR spectra due to the structural transformation in the surface vanadium oxide phase. The Raman spectra of a 1% V_2O_5/TiO_2 sample, possessing a low surface coverage, under ambient and dehydrated conditions are shown in Figure 2. The Raman spectrum of the surface vanadium oxide species under ambient conditions possesses a broad band at ~950 cm^{-1} and the *in situ* Raman spectrum under dehydrated conditions of the surface vanadium oxide species possesses a sharp band at ~1,027 cm^{-1}. The broad Raman band at ~950 cm^{-1} is due to the combination of hydrated metavanadate and decavanadate species[74] and the Raman band observed under dehydration conditions at ~1,027 cm^{-1} is due to the stretching vibration of a terminal vanadium-oxygen double bond, V=O.[31] The structural transformation observed in the Raman spectra upon dehydration of the above 1% V_2O_5/TiO_2 catalyst is also observed in the solid-state ^{51}V NMR spectra. Under ambient conditions, the solid-state ^{51}V NMR spectrum shows that the surface vanadium oxide species exists as a combination of six coordinated (decavanadate) and four coordinated (metavanadate) species as indicated by the wideline chemical shift powder patterns of ~-300 ppm and ~-550 ppm, respectively.[73,74] Upon dehydration of the vanadium oxide supported on titania catalyst, the solid-state ^{51}V NMR spectrum exhibits a chemical shift in the powder pattern at ~-660 ppm due to the surface vanadium oxide species that is anchored to the titania support. Structural transformations from ambient to dehydrated conditions are also observed for surface vanadium oxide species supported on SiO_2, Al_2O_3, Nb_2O_5, and ZrO_2 by Raman spectroscopy and solid-state ^{51}V NMR.[123,132,133] Thus different surface vanadium oxide species are present on these oxide supports for ambient and dehydrated conditions.

An exception to this structural transformation is the V_2O_5/MgO series, where no drastic change occurs between the Raman spectra obtained under ambient and

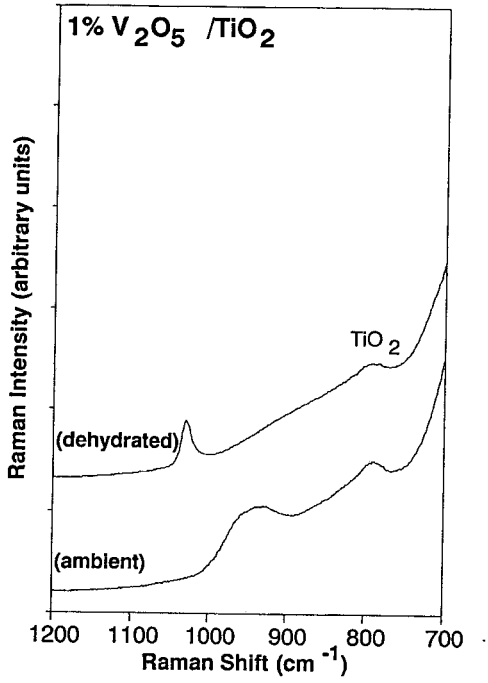

FIGURE 2. Ambient and dehydrated Raman spectra of 1% V_2O_5/TiO_2 monolayer catalyst. Dehydrated spectra obtained at 30°C after heating in oxygen to 400°C for 1 hr. Raman bands at 790 cm^{-1} belong to the TiO_2 support. Raman bands at ~1,030 and ~950 cm^{-1} belong to the surface vanadium oxide species.

dehydrated conditions because vanadium oxide predominantly forms compounds with MgO. Small changes are observed in the adsorption of moisture for the V_2O_5/MgO samples using solid-state ^{51}V NMR, which indicates the presence of small amounts of surface vanadium oxide species.[76] For this reason the V_2O_5/MgO series should not be considered as a monolayer vanadium oxide catalyst since most of the vanadium oxide is present as a bulk compound or solid solution rather than at the surface of the oxide support.

The structure of the surface vanadium oxide species under dehydrated conditions was studied by Raman spectroscopy and solid state ^{51}V NMR. The Raman spectra obtained under dehydrated conditions showed that all the supported vanadium oxide catalysts possessed a single sharp Raman band at 1,016 – 1,037 cm^{-1}, which is assigned to a V=O bond vibration.[31] Furthermore, a broad Raman band is also observed at 840 – 940 cm^{-1} for all the supported vanadium oxide samples (in the 700 – 1,200 cm^{-1} region) with the exception of V_2O_5/SiO_2. The surface vanadium oxide species can be categorized into two groups based on these obser-

vations. The surface vanadium oxide species belonging to the first group exists on SiO_2 and only exhibits the 1,037 cm^{-1} Raman band and an isotropic MAS-NMR chemical shift at ~-710 ppm (wideline chemical shift powder pattern peak maximum at ~-470).[132] The surface vanadium oxide species belonging to the second group exists on Al_2O_3, TiO_2, ZrO_2, and Nb_2O_5 and exhibits two Raman bands at 1,016 – 1,037 and 840 – 940 cm^{-1} (in the 700 – 1,200 cm^{-1} region) and a NMR wideline chemical shift powder pattern peak maximum at ~-660 ppm (MAS-NMR studies in progress).[133]

The structure of the surface vanadium oxide species on SiO_2 (first group) has been recently studied in great detail using Raman and solid-state ^{51}V NMR.[132] These structural characterization studies revealed that a single Raman band due to the surface vanadium oxide species on SiO_2 is present at 1,037 cm^{-1} independent of the vanadium oxide loading, and the isotropic chemical shift in the MAS-NMR for the surface vanadium oxide species is at ~-710 ppm with an axially symmetric line shape. No vanadium-oxygen-vanadium vibrations are observed in the 150 – 250 cm^{-1} region in the Raman spectra, suggesting the absence of a vanadium-oxygen-vanadium functionality. The absence of vanadium-oxygen-vanadium bonds (characteristic of polymeric vanadium oxide species) is also substantiated by dehydrated X-ray absorption studies (EXAFS/XANES) where no vanadium-vanadium neighbor is observed less than 3.5 Å.[84,85] Furthermore, the structure of the surface vanadium oxide species on SiO_2 was unambiguously determined to be a three-legged isolated $(SiO)_3V{=}O$ unit with the aid of model vanadium oxide reference compounds. This isolated surface vanadium oxide species is shown in Figure 3. The presence of a single V=O terminal bond (mono-oxo species) was also confirmed by ^{18}O-^{16}O exchange experiments.[45]

The Raman features observed for the surface vanadium oxide species on Al_2O_3, TiO_2, ZrO_2, and Nb_2O_5 (second group) under dehydrated conditions are somewhat different from the Raman features of the V_2O_5/SiO_2 sample.[123] The Raman spectra of the surface vanadium oxide species on Al_2O_3, TiO_2, ZrO_2, and Nb_2O_5 exhibit two Raman bands, at 1,016 – 1,033 (sharp) and 840 – 940 (broad)

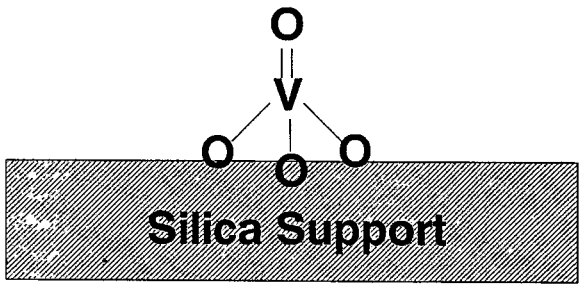

FIGURE 3. Representation of the isolated surface vanadium oxide species on SiO_2.

cm^{-1}, in the 700 – 1200 cm^{-1} region. The intensity ratio of these two bands is a function of the vanadium oxide loading (surface coverage) on these oxide supports. At low vanadium oxide loadings, the sharp Raman band at 1,016 – 1,030 cm^{-1} is dominant, and at monolayer vanadium oxide coverages, the broad Raman band at 840 – 940 cm^{-1} band is of comparable intensity. The changes in relative intensity of these two bands as a function of vanadium oxide loading suggests the presence of two distinct functionalities on these oxide supports corresponding to the 1,016 – 1,033 and 840 – 940 cm^{-1} Raman bands, respectively.

At low vanadium oxide loadings, the 1,016 – 1,030 cm^{-1} Raman band is dominant and the 840 – 940 cm^{-1} Raman band is a minor peak. Thus it can be assumed that the 1,016 – 1,030 cm^{-1} is the only Raman band present under the limiting case of low vanadium oxide loadings. The 1,016 – 1,030 cm^{-1} Raman band is assigned to a V=O bond vibration,[31] which is coincidental with the IR band at 1,029 – 1,040 cm^{-1} for these supported vanadium oxide catalysts. The coincidence of the Raman and IR bands for the terminal V=O bond suggests the presence of a single V=O bond for the surface vanadium oxide species.[58] Furthermore, the surface vanadium oxide species at low coverages is determined to be four coordinated (from solid-state NMR),[74,133] axially symmetric (from solid-state NMR),[74] and isolated (from Raman and EXAFS).[53,84,85] The combination of these data suggests that the surface vanadium oxide species at low coverages on these oxide supports (Al_2O_3, TiO_2, ZrO_2, and Nb_2O_5) is similar to the surface vanadium oxide species shown in Figure 3 and that the difference in the NMR wideline chemical shift powder pattern of vanadium oxide on these oxide supports (~-660 ppm) and on SiO_2 (~-470) may be due to electronic back donation effects. It should be noted that the small shifts in the Raman band positions of the 1,016 – 1033 cm^{-1} band at a particular coverage as a function of the oxide support are due to ~0.01 Å change in bond length of the terminal V=O bond of the surface vanadium oxide species. This suggests that the Raman band position of the terminal V=O vibration is essentially the same and the slight differences in the band positions may arise from differences in oxygen coordination of the oxide support.[50]

In situ Raman spectra obtained under dehydrated conditions as a function of vanadium oxide loading on the Al_2O_3, TiO_2, ZrO_2, and Nb_2O_5 supports reveal that the 840 – 940 cm^{-1} band becomes prominant in comparison with the 1,016 – 1,037 cm^{-1} band on these second group of oxide supports and is assigned to $>V(\doteq O)_2$/-$V(\doteq O)_3$ terminal functionalities.[123] The $>V(\doteq O)_2$/-$V(\doteq O)_3$ terminal functionalities observed are proposed to be protonated to balance the electronic configuration of the terminal oxygen atoms. The two functionalities observed, terminal V=O bond and terminal $>V(\doteq O)_2$/-$V(\doteq O)_3$, are shown in Figure 4. Additional changes are also observed besides the development of the 840 – 940 cm^{-1} Raman band. The V_2O_5/Al_2O_3 system is ideal for studying these changes since the entire 100 – 1,200 cm^{-1} region is readily observed because for this alumina support there are no Raman active modes and the features observed in the Raman spectra belong entirely to the surface vanadium-oxygen vibrations. Conclusions from the V_2O_5/Al_2O_3 system can then be extrapolated to the surface vanadium oxide species on

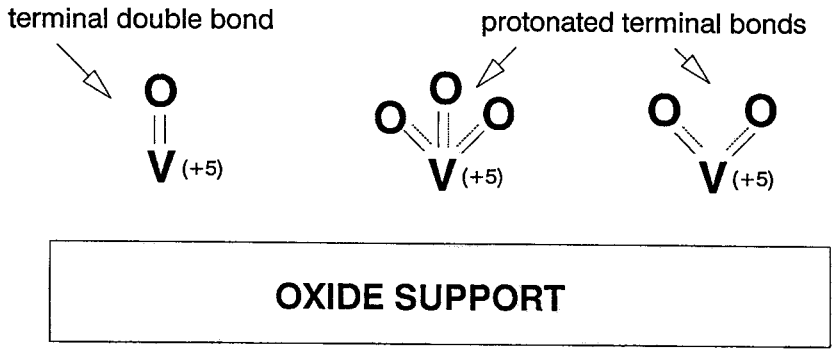

FIGURE 4. Two functionalities observed by Raman spectroscopy on the second group of oxide supports at higher coverages (oxide support = Al_2O_3, Nb_2O_5, TiO_2, and ZrO_2).

the second type of supports (TiO_2, ZrO_2, Nb_2O_5) since the Raman features are essentially identical on these oxide supports.[123]

For high vanadium oxide loadings (15 – 20% V_2O_5/Al_2O_3), Vuurman and Wachs[53] showed that the V=O stretching bond shifts to higher wavenumbers, from 1,016 to 1,025 cm^{-1}, in addition to bands appearing at ~925, ~770, ~620, ~560, ~340, ~250 cm^{-1}. The V=O stretching band (1,025 cm^{-1}) was proposed to arise from a (Support-O-)$_3$V=O species similar to Figure 3, and the additional bands (~925, ~770, ~620, ~560, ~340, ~250 cm^{-1}) were assigned to a polymeric species.[53] The presence of a (Support-O-)$_3$V=O species has also previously been proposed.[40,47,51,74,84,85,94,123] Polymeric vanadium oxide species at higher vanadium oxide loadings were also proposed by Went et al. [47,52] for V_2O_5/TiO_2 catalysts (based only on the Raman bands in the 700 – 1,200 cm^{-1} region) and V_2O_5/Al_2O_3 catalysts (based on the Raman bands in the 400 – 1,200 cm^{-1} region). Vuurman et al.[51] also proposed the presence of polymeric vanadium oxide species for V_2O_5/TiO_2 samples based on the Raman bands in the 700 – 1,200 cm^{-1}. The presence of polymeric vanadium oxide species proposed in some of these studies was concluded from the presence of the 840 – 940 cm^{-1} Raman band, which is typical of metavanadate species. However, the 840 – 940 cm^{-1} Raman band should not be considered as identification of polymeric species since these bands can also arise from terminal >V(=O)$_2$/-V(=O)$_3$ functionalities. Polymeric vanadium oxide species must contain vanadium-oxygen-vanadium linkages, which should give rise to Raman bands at 200 – 250 cm^{-1} (V-O-V bending), 475 – 573 cm^{-1} (V-O-V asymmetric stretching), and 630 – 815 cm^{-1} (V-O-V symmetric stretching).[123] Only the study of Vuurman and Wachs[53] observes and assigns all these bands. Recent studies show that Raman bands less than 250 cm^{-1} are not directly evident on a different V_2O_5/γ-Al_2O_3 sample,[123] which suggests that the observation of polymeric vanadium oxide species is not always straightforward. The uncertainties in observing Raman bands due to V-O-V functionalities (necessary for positive

identification of polymeric species) may be due to weak and broad bands usually associated with vibrations in this region.

Additional information from other characterization techniques is necessary to clarify the assignment of the 840 – 940 cm^{-1} Raman band. Wideline solid-state ^{51}V NMR powder patterns for the surface vanadium oxide species on Al_2O_3, TiO_2, ZrO_2, and Nb_2O_5 are similar (~-660 ppm), and no changes are observed as a function of vanadium oxide loading.[133] Solid-state NMR is apparently not as sensitive as vibrational spectroscopy to subtle changes and the changes observed by Raman spectroscopy may not be readily detected by NMR. *In situ* IR spectroscopy of monolayer supported vanadium oxide catalysts (V_2O_5/TiO_2, V_2O_5/ZrO_2, and V_2O_5/Al_2O_3) show the presence of a band at 1,029 – 1,042 cm^{-1} corresponding to the V=O terminal bond vibration,[34,42,46,48,59] but additional vibrations below 950 cm^{-1} were not detected since the vibrations of the oxide supports (Al_2O_3, TiO_2, and ZrO_2) dominate this region (<1000 cm^{-1}).[58] *In situ* X-ray absorption studies (XANES/EXAFS) of high vanadium oxide surface coverages on oxide supports are not available in the literature. Recent *in situ* diffuse reflectance spectroscopy (DRS) studies of the V_2O_5/Al_2O_3 system as a function of the vanadium oxide loading reveal the development of a spectral feature at ~310 nm (polymeric species) at monolayer vanadium oxide loadings, in addition to a band at ~275 nm (monomeric species), which suggest the presence of a second surface vanadium oxide structure.[99] However, additional experiments are required to clarify the assignments of these diffuse reflectance spectral changes as a function of vanadium oxide loading. Thus the second Raman feature at 840 – 940 cm^{-1}, which is prominant at high vanadium oxide loadings on the second group of supports (Al_2O_3, TiO_2, ZrO_2, and Nb_2O_5), is not complemented by other spectroscopic techniques, and the exact nature of the second functionality is not completely certain at present. Despite this ambiguity, it is evident that essentially two distinct types of surface vanadium oxide functionalities exist on the Al_2O_3, TiO_2, ZrO_2, and Nb_2O_5 supports. At present, these two types of functionalities are represented as isolated and polymeric surface vanadium oxide species in accordance with previously proposed studies and are shown in Figure 5.

In summary, the Raman spectra of the dehydrated supported vanadium oxide catalysts reveals that the structure of the surface vanadium oxide species is essentially identical on TiO_2, ZrO_2, Al_2O_3, and Nb_2O_5 and possesses a combination of terminal V=O and $>V(=O)_2$/-$V(=O)_3$ functionalities with similar ratios at a particular vanadium oxide coverage. For the dehydrated silica supported vanadium oxide catalysts, the surface vanadium oxide species are isolated and only possess a terminal V=O bond.

C. Influence of Synthesis Methods

Many different synthesis methods have been used in the preparation of supported metal oxide catalysts because the state of dispersion of the supported metal

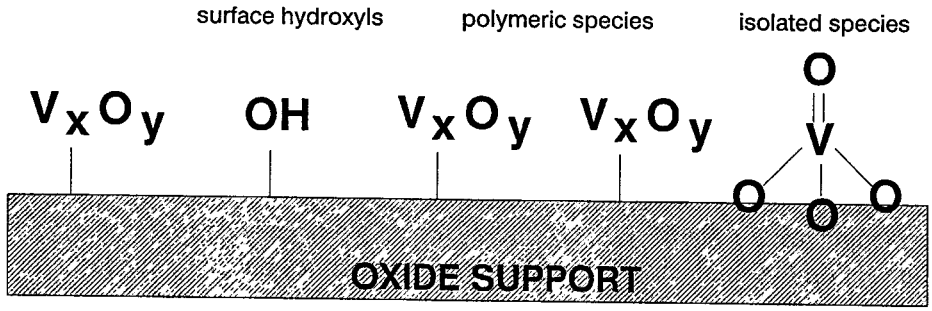

FIGURE 5. Representation of surface vanadium oxide species (isolated and polymeric) at monolayer coverages (oxide support = Al_2O_3, Nb_2O_5, TiO_2, and ZrO_2; see text).

oxide component plays a critical role in catalytic reactions. In the case of supported V_2O_5/TiO_2 catalysts, catalysts were prepared by vapor phase grafting with $VOCl_3$,[82,134] nonaqueous impregnation of vanadium alkoxides[39] and vanadium acetate,[135] aqueous impregnation of vanadium oxalate,[136] as well as dry impregnation with crystalline V_2O_5 (thermal spreading).[137] Commercial preparations usually employ aqueous impregnation with vanadium oxalate because of its high solubility in water and the absence of volatile solvents, which are potentially combustible. However, some researchers have claimed that certain preparations result in superior catalytic properties.[134]

A series of V_2O_5/TiO_2 catalysts possessing high vanadium oxide loadings, 4 – 6 wt. % V_2O_5, were prepared by the different synthesis methods mentioned above and characterized with Raman spectroscopy to determine the influence of the various synthesis methods.[138] Raman analysis of the hydrated catalysts exhibited a band at ~990 cm^{-1}, which is characteristic of hydrated decavanadate on all the catalysts (also confirmed by solid-state ^{51}V NMR studies). The one exception was the catalysts prepared by impregnation with crystalline V_2O_5 via spontaneous spreading that still possessed some crystalline V_2O_5 particles, in addition to the surface decavanadate species, because much longer calcination times are required to completely disperse the crystalline precursor (see additional discussion below). The presence of hydrated decavanadate species on all these V_2O_5/TiO_2 catalysts analyzed under ambient conditions is consistent with the relatively low surface pH at pzc for these high vanadium oxide loaded catalysts (~4).[125] Furthermore, the same surface pH at pzc for all the catalysts suggests that the preparation method cannot influence the specific hydrated surface vanadium oxide system, which is in equilibrium with its aqueous environment.

The above series of samples that were synthesized by different methods were also examined with *in situ* Raman spectroscopy under dehydrated conditions.[138] Upon dehydration, all the V_2O_5/TiO_2 catalysts exhibited the same Raman bands (sharp feature at ~1,030 cm^{-1} and broad features at ~930 cm^{-1}), suggesting that the same surface vanadium oxide species were present in all the samples. Solid-state ^{51}V NMR measurements also substantiate this conclusion. The one exception was

the sample prepared by spontaneous dispersion that still possessed some residual crystalline V_2O_5 in addition to the surface vanadium oxide species due to the somewhat slow surface diffusion rates of this crystalline phase under the calcinations conditions employed. The fact that the spontaneous dispersion preparation method, which is a dry impregnation procedure, results in the same surface vanadium oxide species demonstrates that all preparation methods give the same thermodynamically stable species. Thus the preparation methods appear to have no influence on the final surface vanadium oxide structures on TiO_2, but can affect (delay) the process of their formation, as in the case of dry impregnation (thermal spreading), due to thermodynamic and surface mobility factors involved.

Detailed comparative synthesis studies have not been performed with other supported vanadium oxide systems (e.g., alumina, silica, niobia). The above studies, however, suggest that the same results should occur on all oxide supports and should be independent of the specific synthesis method. Thus for hydrated surface vanadium oxide systems, the structures are determined by the net surface pH at pzc of the aqueous thin film[49] and the same thermodynamically stable dehydrated surface species are formed on all the oxide supports.[47,123] The one exception to the above situation occurs when there is a potential for solid solution formation between the surface vanadium oxide species and the oxide support (e.g., V_2O_5/MgO). In such instances, the precalcination of the oxide support as well as the calcination temperature can become a critical parameter[123,139] Furthermore, the dispersion of metal oxides on hydrophobic oxide supports such as SiO_2 can be increased by certain nonaqueous preparations, but such preparations still result in the same surface metal oxide species.[128]

The thermal spreading of vanadium oxide has recently attracted much attention[140] and is discussed only briefly here. Thermal spreading occurs when an active solid component of an oxide catalytic system undergoes thermal pretreatment in the presence of another solid (e.g., an oxide playing the role of the support). The minority oxide (supported phase) can accumulate entirely at the surface of another oxide (support) when the temperature of annealing is low enough and the miscibility as well as chemical affinity of the two oxides is very limited. In the case of miscibility of the two oxide phases, a solid solution can be formed at a high enough temperature, and in case of chemical affinity of the two oxides, new surface or bulk compounds can be synthesized. Pentavalent vanadium oxide shows acidic properties and its chemical affinity to such supports as titania, alumina, and silica is negligible at modest temperatures, and it remains, therefore, at the surface of these supports retaining its chemical identity and forming an overlayer.[141–144]

Spontaneous spreading of V_2O_5 occurs over the surface of these oxide supports as the manifestation of the wetting of one solid by another solid due to the operation of the forces of surface tension since the surface free energy of crystalline V_2O_5 is much lower than supports such as Al_2O_3, SiO_2, and TiO_2[143] and the Tammann temperature of V_2O_5 is low (428 K).[141,142] For amounts of V_2O_5 in excess of that required for monolayer loading, spreading should continue until the formation of a thermodynamically stable vanadium oxide overlayer characterized by a

surface free energy equal to that of the bulk oxide support. The difference in surface free energy between the migrating phase and the oxide support is the condition necessary for surface spreading to occur, but not sufficient since the surface mobility obviously imposes kinetic limitations on this phenomenon. The behavior of such systems as V_2O_5-MgO, however, is different because of the high chemical affinity of these two oxides that results in nucleation of new compounds instead of spreading of vanadia over the surface of MgO.

D. Influence of Additives on the Dehydrated Surface Vanadium Oxide Structures

Typically, the properties of supported vanadium oxide catalysts are modified by the addition of impurities/promoters.[5] There are various ways that impurities/promoters can interact with the surface vanadium oxide species.[51] The impurities/promoters can interact: (1) directly with the surface vanadium oxide species and form new surface species or crystalline phases, (2) with the oxide support and change the surface vanadium oxide species due to lateral interactions, or (3) with the oxide support without changing the surface vanadium oxide species.

To examine the effect of promoters, a series of promoters (tungsten oxide, niobium oxide, silica, potassium oxide, and phosphorous oxide) were added to a 1% V_2O_5/TiO_2 catalyst. The influence of the different promoters upon the structure of the surface vanadium oxide species was examined with Raman spectroscopy, and the results are presented in Table 7. The addition of tungsten oxide, niobium oxide, and silica did not affect the structure of the surface vanadium oxide species since the V=O bond due to the surface vanadium oxide species is essentially unchanged. The slight Raman changes reflect the net higher surface coverages and lateral interactions in the over layer (cases 2 and 3 above). However, the addition

TABLE 7
Raman Band Position for Promoters on 1%V_2O_5/TiO_2

Promoters on 1% V_2O_5/TiO_2	Raman band positions (700–1200 cm^{-1} region)
None	1,027
6% Nb_2O_5	1,031, 928
3% SiO_2	1,024
7% WO_3	1,031, 925
0.3% K_2O	1,023, 997
0.7% K_2O	1,009,[a] 980
3% P_2O_5	1,035, 925

[a] Weak.

of potassium oxide and phosphorous oxide had a significant effect on the structure of the surface vanadium oxide species (case 1 above). The addition of potassium oxide dramatically decreases the position of the Raman band from 1,027 to 980 cm^{-1} (corresponding to an increase in the vanadium-oxygen bond length), and the addition of phosphorous oxide results in the formation of crystalline α_1-$VOPO_4$ (1,035, 925 cm^{-1}).[145] The effect of impurities/promoters at higher surface coverages of vanadium oxide appear to follow the same trend and similar results were also observed when using other supports. Thus the influence of certain promoters on the structure of surface vanadium oxide species can be significant (e.g., potassium and phosphorous).

E. Effect of Moisture on Dehydrated Surface Vanadium Oxide Structures

Previous sections discuss how the structure of the surface vanadium oxide species is different under ambient and dehydrated conditions due to the adsorption of significant amounts of moisture under ambient conditions. In practice, supported vanadium oxide catalysts are employed at elevated temperatures where moisture is either present in the feed or generated from partial oxidation reactions (see part V on reactivity).

The effect of moisture on the surface vanadium oxide structure under *in situ* conditions was recently examined by flowing an oxygen stream containing ~8% H_2O over 1% and monolayer loading supported vanadium oxide catalysts at elevated temperatures (175 – 500°C).[146] The changes in the structure of the surface vanadium oxide species were monitored by *in situ* Raman spectroscopy starting with the completely dehydrated surface vanadium oxide structure at 500°C. The effect of moisture on the vanadium oxide structure on different oxide supports was essentially similar with the exception of the V_2O_5/SiO_2 catalyst. At 500°C no significant changes in the *in situ* Raman spectra were observed irrespective of the vanadium oxide loading, and consequently, the surface vanadium oxide structure remained essentially the same. The only change observed under these conditions was that the Raman band for the V=O bond shifted down ~2-3 cm^{-1} due to hydrogen bonding with some small amounts of moisture. This shift reveals that some moisture is present on the catalyst surface at elevated temperatures. At temperatures significantly below 300°C, the intensity of the Raman bands due to the surface vanadium oxide species for all vanadium oxide loadings progressively decreased and became broader due to the adsorption of additional moisture. Ultimately, decreasing the temperature below 200°C resulted in *in situ* spectra similar to the Raman spectra obtained under ambient conditions, which suggests that a thin aqueous layer is being formed. For the V_2O_5/SiO_2 catalyst, however, no change in the Raman spectra is observed in the 500 to 175°C range due to the hydrophobic nature of silica. Thus it appears that water coordinated to the surface vanadium oxide species and decreases the number of available surface vanadium

oxide sites on all the supported vanadium oxide catalysts by blocking these sites. The coordination of water molecules to the exposed oxide support surface probably also occurs, but could not be monitored with Raman spectroscopy. This observation accounts for the negative effect of moisture on the reactivity of supported vanadium oxide catalysts during oxidation reactions and shows that the magnitude of this effect increases with decreasing temperatures.

F. Summary

The surface vanadium oxide structures under ambient conditions closely follow the vanadium(V) ion behavior in aqueous solutions, and consequently, the structure of the surface vanadium oxide species is controlled by the net surface pH at pzc. Under dehydrated conditions, the surface vanadium oxide species bonds directly with the oxide support surface and two types of surface vanadium oxide species are observed. The first type occurs on SiO_2 where an isolated, three-legged $(SiO)_3V{=}O$ species is present at all loadings. The second type of surface vanadium oxide species exists on TiO_2, ZrO_2, Al_2O_3, and Nb_2O_5 where two distinct types of functionalities exist: corresponding to a terminal V=O bond and terminal $>V(\text{-}O)_2$/ $\text{-}V(\text{-}O)_3$) bonds. These vary as a function of loading with the terminal V=O bond predominantly present at low loadings and the terminal $>V(\text{-}O)_2$/$\text{-}V(\text{-}O)_3$) functionality is present at comparable abundance at high loadings. Additional experiments need to be performed to characterize completely the second type of surface vanadium oxide species. Additives/impurities either interact with the surface vanadium oxide species by changing its structure or preferentially interact with the oxide support, which leaves the surface vanadium oxide species and structure almost unchanged under dehydrated conditions. Moisture decreases the number of available surface vanadium oxide sites on all the supported vanadium oxide catalysts, except the V_2O_5/SiO_2 system where no change is observed.

V. REACTIVITY OF VANADIUM OXIDE MONOLAYER CATALYSTS

The reactivity of supported vanadium oxide catalysts has been examined for several catalytic reactions (e.g., the oxidation of o-xylene, 1,3-butadiene, methanol, carbon monoxide, ammoxidation of aromatic hydrocarbons (toluene and 3-picoline), selective catalytic reduction (SCR) of nitric oxide, and partial oxidation of methane).[1,2] Most of these studies have revealed the unique reactivity properties of the surface vanadium oxide phase. Some of the reactions involving vanadium oxide monolayer catalysts are discussed below with regards to the structural information discussed in part IV. The oxidation of methanol is addressed first due to its simplicity. Progressively more complicated reactions are then discussed in order systematically to develop a better fundamental understanding of the reactivity of the surface vanadium oxide species.

A. Methanol Oxidation

The methanol oxidation reaction was used as a chemical probe to study the reactivity of the surface vanadium oxide species. The product selectivity of the methanol oxidation reaction reflects the reaction pathways that depend on the acidic, basic, or redox sites present on the catalyst surface. For example, acidic sites present on the surface of catalysts give rise to dimethyl ether, basic sites produce essentially carbon oxides (CO and CO_2), and redox sites (sites able to undergo reduction-oxidation cycles) produce formaldehyde, methyl formate, and dimethoxymethane. At high conversions, the reaction products from the acidic and redox sites can also be further oxidized to yield carbon oxides. These three reaction pathways for the partial oxidation of methanol are relatively independent at low conversions and have been successfully used to probe the presence of the various types of sites present on the surface of oxide catalysts.[50,61,62,102,139,147-150]

Formaldehyde is the primary product for the various supported vanadium oxide catalysts used in the present study (1 wt. % V_2O_5 loading). The only exception is the V_2O_5/Al_2O_3 catalyst system, where the primary product was dimethyl ether, and only trace amounts of formaldehyde were formed. The large selectivity toward dimethyl ether for the 1% V_2O_5/Al_2O_3 catalysts is due to the high reactivity of the exposed alumina Lewis acid sites.[70] Therefore, the partial oxidation products were used to calculate the reactivity of the surface vanadium oxide species on alumina. The activity of the V_2O_5/SiO_2 catalysts was low and of the same order as the SiO_2 support, but the formation of partial oxidation products (formaldehyde - 72%), instead of carbon oxides, indicates that the oxidation products arise from the surface vanadium oxide species. The remaining oxide supports (TiO_2, ZrO_2, and Nb_2O_5) are essentially inactive relative to the activity of the supported vanadium oxide catalysts. The primary formaldehyde product from the surface vanadium oxide species makes it possible to compare the reactivity of the redox sites formed by the surface vanadium oxide species on different oxide supports.

In part IV, it was concluded that only molecularly dispersed vanadium oxide species are present on the different oxide supports at low loadings, and consequently, the methanol oxidation activity can be normalized per vanadium atom (the turnover frequency - TOF). Normalizing the reaction rate with respect to the vanadium atoms inherently assumes that all the surface vanadium oxide species participate equally in the reaction. The TOFs of the different supported vanadium oxide catalysts (1 wt. % V_2O_5) are given in Table 8. Comparison of the reactivity of the surface vanadium oxide species on the different oxide supports in Table 8 reveals that the TOF varies by three orders of magnitude. The TOF of vanadium oxide supported on TiO_2 and ZrO_2 are three orders of magnitude greater than the TOF for vanadium oxide supported on SiO_2. Vanadium oxide supported on Nb_2O_5 is slightly less reactive than vanadium oxide on ZrO_2 and TiO_2. The redox TOF of vanadium oxide supported on Al_2O_3 is close to that of bulk V_2O_5 and the TOF of V_2O_5/SiO_2 is one order of magnitude lower than that of bulk V_2O_5. The two to three orders of magnitude difference in TOF occurs even though essentially the same

TABLE 8
TOF of Different Supported Vanadium Oxide Catalysts at Low Loadings (1 wt. % V_2O_5)

Oxide support	TOF (sec^{-1})
SiO_2	$3.9 * 10^{-3}$
γ-Al_2O_3	$3.6 * 10^{-2}$
Nb_2O_5	$8.0 * 10^{-1}$
TiO_2	$2.0 * 10^{0}$
ZrO_2	$3.3 * 10^{0}$

surface vanadium oxide species (characterized by the ~1,030 cm^{-1} band in the Raman spectra and the ~-660 ppm peak in the solid-state ^{51}V NMR spectra) is present on the different dehydrated oxide supports. The implication of this conclusion is of fundamental and practical importance since the difference in reactivity of the surface vanadium oxide species on different oxide supports is not due to a structural factor as previously proposed.[1]

The effect of vanadium oxide loading on the activity and selectivity for a series of V_2O_5/TiO_2 catalysts was probed with the methanol oxidation reaction. The primary reaction product is formaldehyde and is formed with a selectivity in excess of 95%. This makes it possible to compare the effect of loading of vanadium oxide on the titania support without having the complication of dealing with multiple reaction pathways. The activity per gram of catalysts for vanadium oxide supported on the titania is presented in Figure 6 and shows that the methanol oxidation activity increases monotonically as a function of vanadium oxide loading.

Similar increases in methanol oxidation activity as a function of vanadium oxide loading are also observed for vanadium oxide supported on ZrO_2, Nb_2O_5, Al_2O_3, and SiO_2. Conversion of the activity to TOF of the partial oxidation products reveals that there is a small initial increase and then a slight decrease in the TOF for this series of supported vanadium oxide catalysts. However, there is no correlation between the change in TOF and the apparent variation of the Raman signals of the two species (isolated and polymeric species) in Figure 5. This slight variation in TOF as a function of vanadium oxide loading is most probably due to experimental error associated with obtaining the oxidation activity data and is within a factor of 2.5. Similar reactivity patterns for vanadium oxide supported on different oxides (Al_2O_3, ZrO_2, Nb_2O_5, and SiO_2) were also observed with increasing vanadium oxide loadings.[139]

The TOFs for the partial oxidation of methanol over monolayer vanadium oxide catalysts on different oxide supports are presented in Table 9. The TOFs of the various supported vanadium oxide species vary by three orders of magnitude as one goes from the vanadium oxide species on TiO_2 and ZrO_2 compared to SiO_2.

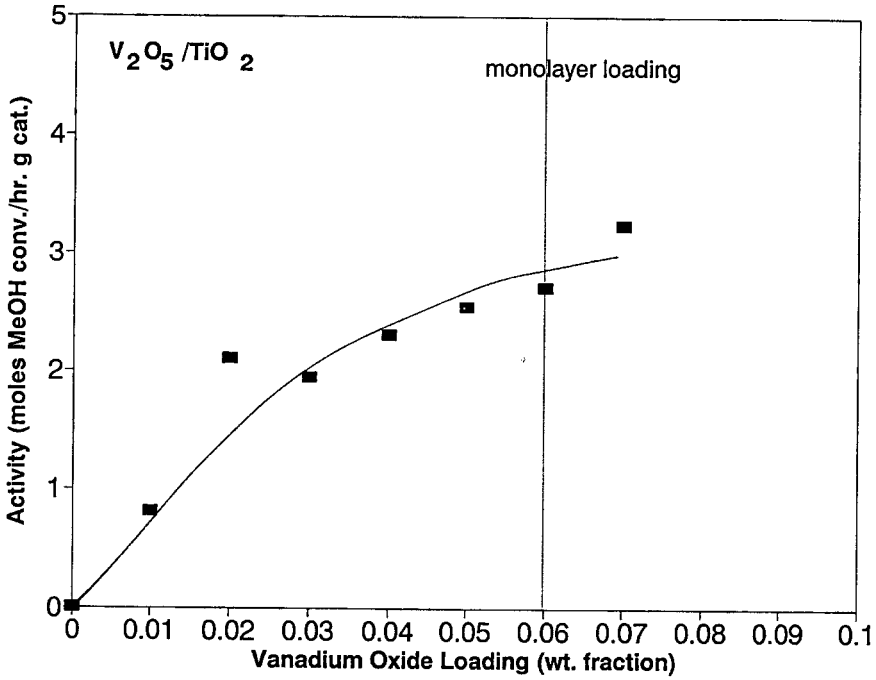

FIGURE 6. Methanol oxidation activity over V_2O_5/TiO_2 catalysts as a function of V_2O_5 weight fraction. Monolayer loading shown at 0.06 weight fraction V_2O_5.

This variation of TOF for the supported vanadium oxide species at monolayer coverage is similar to the variation observed in Table 8 for low loadings. Thus the reactivity of supported vanadium oxide catalysts for the reaction of methanol to formaldehyde is independent of changes in the structure of the surface vanadium oxide species and just requires the presence of a single surface vanadium oxide site (structure insensitive reaction).

TABLE 9
TOF of Different Supported Vanadium Oxide Catalysts at Monolayer Loadings

Oxide support	wt. % V_2O_5	TOF (sec^{-1})
SiO_2	3	$3.1 * 10^{-3}$
γ-Al_2O_3	20	$6.8 * 10^{-2}$
Nb_2O_5	7	$4.0 * 10^{-1}$
TiO_2	6	$1.1 * 10^{0}$
ZrO_2	4	$1.7 * 10^{0}$

Comparison of the reactivity of the supported vanadium oxide catalysts with the Raman band positions of the terminal V=O bonds reveals that no correlation exists.[55] The Raman frequency of a vanadium oxygen bond is related to its bond strength.[31] From this relationship, the Raman frequencies of the terminal V=O bonds of the different supported vanadium oxide catalysts (Tables 8 and 9) are converted to bond strengths and plotted versus the respective TOFs in Figure 7.

It is evident from Figure 7 that no relationship exists between the terminal V=O bond strength and the reactivity in the methanol oxidation reaction. Furthermore, two catalysts possessing approximately the same V=O bond strength exhibit TOFs that differ more than an order of magnitude, which also suggests that there is not an optimum V=O bond strength (e.g., volcano effect). This is in direct contradiction to the proposal that the oxidation activity correlates with the strength of the terminal V=O bond.[1] The independence of the terminal M=O bond strength with respect to reactivity is also observed for other surface metal oxide species.[55] Thus the reactivity of the supported vanadium oxide catalysts is not related to the strength of the terminal V=O bond and consequently, is apparently related to the vanadium-oxygen-support (V-O-S) bond.

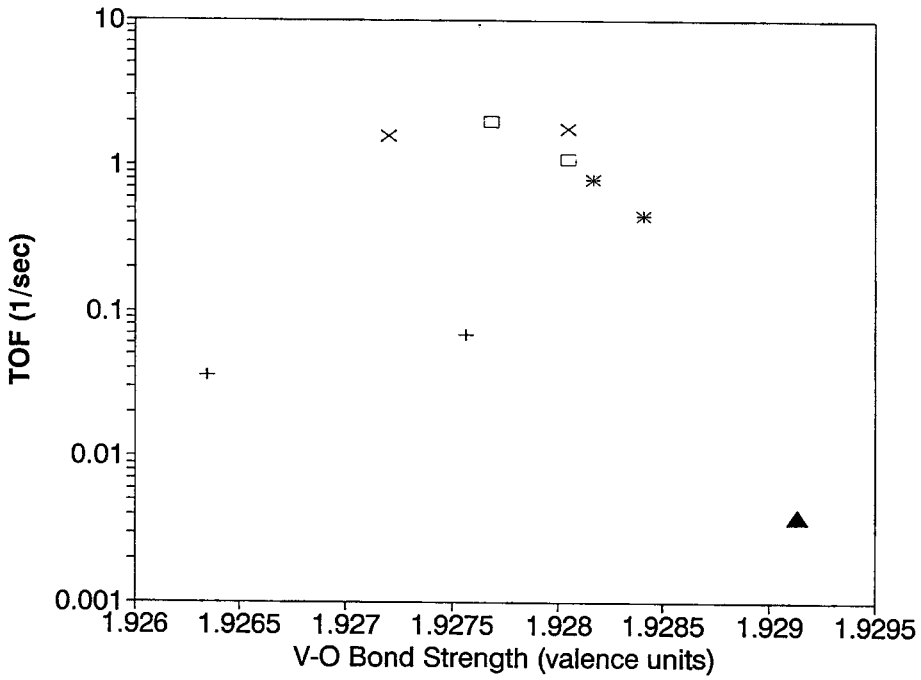

FIGURE 7. Variation of methanol oxidation TOF with V=O bond strength for supported vanadium oxide catalysts. Bond strength of V=O terminal bond calculated from Raman band position using ref. 31. Δ – V_2O_5/SiO_2; + – V_2O_5/Al_2O_3; * – V_2O_5/Nb_2O_5; □ – V_2O_5/TiO_2; × – V_2O_5/ZrO_2.

Additional kinetic information about the surface vanadium oxide species was obtained from activation energy studies. The activation energy for formaldehyde formation by the different supported vanadium oxide catalysts was found to be 19.6 ± 2.3 kcal/mole, which is typical of C-H bond breaking of the surface methoxide intermediate species which forms formaldehyde.[151-153] The similar activation energy for the partial oxidation of methanol over the surface vanadium oxide species implies that the difference in the reaction rates of the various supported vanadium oxide catalysts is associated with differences in the pre-exponential factor. The structure insensitivity of the methanol oxidation reaction over the supported vanadium oxide catalysts suggests that the differences in the pre-exponential factor are most probably related to the number of active sites and/or the activity per site.

In situ Raman experiments during methanol oxidation were carried out over the supported vanadium oxide catalysts during the methanol oxidation reaction in order to obtain further insight into the origin of the differences in the pre-exponential factor. It was observed that the fraction of surface vanadium oxide species participating in the reaction for the different supported vanadium oxide catalysts were similar irrespective of the specific oxide support. The fraction of surface vanadium oxide species participating in the reaction was determined from the decrease in the intensity of the ~1,030 cm^{-1} Raman band (due to the reduction of V^{+5}). The similar amounts of surface vanadium oxide species participating in the reaction implies that the number of active sites are the same over the various supported vanadium oxide catalysts during methanol oxidation. Thus the differences in pre-exponential factors for the supported vanadium oxide sites appear to depend strongly on the activity per site. Additional studies are underway to determine the nature of the activity per site for the different supported metal oxide catalysts. Recent molecular orbital calculations suggest that the oxide support might exert an indirect influence on the pre-exponential factor during methanol oxidation by contributing to the density of unoccupied orbitals of the catalyst, which factors into the entropy of activation or the activity per site.[154]

Additional insight into the fundamental factors affecting the reactivity of supported vanadium oxide catalysts was obtained from temperature programmed reduction (TPR) experiments and the T_{max} temperatures are presented in Table 10. The T_{max} temperatures in Table 10 were determined by measuring the weight loss as a function of increasing temperature in a hydrogen environment using a Cahn microbalance. Similar trends in T_{max} temperature have been reported by Roozeboom et al. and Nickl et al. as a function of oxide support.[101,102,155] Comparison of the T_{max} temperatures and the TOFs for methanol oxidation reveals that a decrease in T_{max}, more reducible vanadium oxide, results in an increase in the TOF. Furthermore, the T_{max} temperature is directly related to the surface reducibility of the pure oxide supports without vanadium oxide. The TiO_2 and Nb_2O_5 supports are reducible oxides and ZrO_2 is known readily to reduce at the surface.[156,157] The Al_2O_3 and SiO_2 supports, however, are not reducible. Relating these two reduction characteristics, the oxide sup-

TABLE 10
T_{max} Temperature Determined from TPR Experiments for Monolayer Supported Vanadium Oxide Catalysts

Vanadium oxide catalysts	wt. % V_2O_5	T_{max} (°C)
SiO_2	3	774
γ-Al_2O_3	20	675
Nb_2O_5	7	ND
TiO_2	6	620
ZrO_2	4	600

ND = not determined.

ports and the supported vanadium oxide catalysts, suggests that the reduction process is kinetically controlled by the V-O-S bond. The importance of the V-O-Support bond is also evident in the enhanced reactivity of vanadium oxide supported on a surface titania modified silica support[158] and is substantiated by comparing the reactivity of supported MoO_3, CrO_3, and Re_2O_7 catalysts, which also follow similar trends in TOF as a function of oxide support.[55] Relating the V-O-Support characteristics and the TOF suggests that the pre-exponential factors of the different supported vanadium oxide catalysts are directly related to the reducibility of the V-O-Support bond: a less reducible V-O-Support bond would imply a smaller pre-exponential factor and a more reducible V-O-Support bond would imply a larger pre-exponential factor at steady state. In conclusion, the oxide support appears to act as a ligand that influences the reactivity of surface metal oxide overlayers.

B. Carbon Monoxide Oxidation

The reactivity of monolayer vanadium oxide supported catalysts was also examined for carbon monoxide oxidation to carbon dioxide as a function of the oxide support.[101] The reaction was proposed to occur via a redox mechanism with the reduction step as the rate determining step. The specific oxide support was found to influence the reactivity of the surface vanadium oxide overlayer and decreased in the following order: $ZrO_2 > TiO_2 > CeO_2 > Al_2O_3$. The exact same trend was also found by the same investigators for methanol oxidation activity over these supported vanadium oxide catalysts.[102] In addition, the reactivities of these vanadium oxide monolayer catalysts for carbon monoxide and methanol oxidation were directly related to the trends in reducibility observed in TPR experiments. Thus the more easily reducible catalysts were more active in the oxidation

reaction. The results of the V_2O_5/CeO_2 catalyst in these investigations were marred by compound formation between vanadia and ceria. The influence of surface vanadium oxide coverage on carbon monoxide oxidation has not been investigated to date, but the reactivity of the oxide supports for CO oxidation would complicate such an analysis.[159] The carbon monoxide oxidation studies confirm that the specific oxide support has a pronounced effect on the reactivity of the monolayer vanadium oxide catalysts, and the exact same trends are observed as for methanol oxidation.

C. Sulfur Dioxide Oxidation

The oxidation of sulfur dioxide to sulfur trioxide is a well-established commercial process for the manufacture of sulfuric acid. This reaction is conducted over silica-supported vanadium oxide catalysts that are promoted by potassium pyrosulfate.[4] Kinetics of the reaction indicate that the reaction is about first order with respect to oxygen concentration, has a positive dependence on sulfur dioxide concentration, and is inhibited by sulfur trioxide concentration. The kinetics also have a positive dependence on the vanadium oxide content of the catalyst. However, the vanadium oxide in these catalysts is not present as a two-dimensional overlayer, but is present as a liquid melt in the pores of the silica support under the conditions of the reaction. Conseqently, commercial sulfuric acid catalysts are not discussed here.

The oxidation of sulfur dioxide to sulfur trioxide also occurs during many reactions involving monolayer vanadium oxide catalysts when sulfur dioxide is present in the reactant stream. For example, sulfur dioxide is present in the NO_x containing flue gases from stationary emissions, which are selectively reduced with ammonia over a vanadium oxide monolayer on a titania support.[160–162] In these applications, especially the selective catalytic reduction of NO_x, it is critical that the amount of sulfur trioxide is minimized because it reacts with ammonia to form ammonium sulfates that cause engineering problems with heat exhangers. However, an examination of the literature reveals that little information exists about the kinetics of the sulfur dioxide oxidation reaction over supported vanadium oxide catalysts (effects of oxide support, vanadium oxide concentration, and reactant gas partial pressures). It is anticipated that the specific oxide support should have a pronounced effect on the reactivity of the vanadium oxide monolayer catalyst. It is hoped such information will be generated in the next few years because of the importance of this reaction in pollution control strategies.

D. O-Xylene Oxidation

There has been much interest in the catalytic oxidation of o-xylene to phthalic anhydride because of the commercial importance of this reaction. The commercial

catalyst consists of vanadium oxide supported on titania with the addition of several promoters to enhance the catalyst selectivity.[5,163] Fundamental studies combining structural information from Raman spectroscopy and reactivity data have revealed that the vanadium oxide monolayer on the titania support is the active site for this reaction and that crystalline V_2O_5 is less active and selective.[136] Furthermore, the selective oxidation of the more complex o-xylene molecule requires that the titania support be completely covered by the vanadium oxide overlayer since exposed titania sites result in undesirable side reactions that lead to complete combustion. As a consequence of the detrimental influence of exposed titania sites upon o-xylene oxidation, both the catalyst reactivity and selectivity increase with surface vanadium oxide coverage until monolayer loadings is achieved. At vanadium oxide loadings exceeding monolayer coverages, there is very little change in catalyst activity and selectivity because the crystalline V_2O_5 phase is significantly less active than the vanadium oxide monolayer on titania. Simultaneously, a decrease in acidity, as measured by the probe reaction of isopropanol, is observed as a function of vanadium oxide coverage.[164] Thus it is critical to compare supported vanadium oxide catalysts for o-xylene oxidation only at monolayer or higher coverages. The calcination temperature is also a critical parameter since the vanadium oxide monolayer requires a minimum temperature for its formation, ~350°C and can be destroyed by solid-state reactions with the titania support at elevated temperatures, > 575°C.[37,163] These studies with o-xylene oxidation demonstrate the important influence of the vanadium oxide monolayer during catalysis over titania supported vanadium oxide catalysts.

The influence of the specific oxide support upon the reactivity of supported vanadium oxide catalysts for o-xylene oxidation was also investigated.[165] The best catalytic performance was obtained with a TiO_2 support followed by SnO_2 and ZrO_2. These results reveal that the oxide support has a dramatic effect on the catalysis of vanadium oxide monolayers employed for o-xylene oxidation and is consistent with the general finding that the specific oxide support controls the catalytic properties of the vanadium oxide overlayer. The oxide supports exhibiting superior catalytic performance again correspond to oxides that are reducible (TiO_2, ZrO_2, and SnO_2). Vanadium oxide on other oxide supports (Al_2O_3, MnO_2, Nb_2O_5, and SiO_2) were determined to be ineffective for o-xylene oxidation. However, particulars for the oxide supports and details of the reaction rate were not mentioned and a detailed analysis (e.g., why Nb_2O_5 was ineffective as an oxide support) could not be performed for this series of catalysts.

The influence of the preparation method upon the properties of vanadium oxide monolayer titania catalysts for o-xylene oxidation was also investigated by several research groups.[166–168] Bond and Konig[166] studied V_2O_5/TiO_2 (anatase) catalysts prepared by grafting ($VOCl_3$) and impregnation (vanadium oxalate) for the oxidation of o-xylene. They observed that the catalysts prepared by grafting gave a higher yield and selectivity for phthalic anhydride compared to catalysts prepared by impregnation. However, the reactivity data did not correlate with corresponding TPR measurements, which gave identical results for the catalysts

prepared by grafting and impregnation.[103] In contrast, Cavani et al.[168] concluded that there are no significant differences between grafting and impregnating V_2O_5/TiO_2 (anatase) catalysts for o-xylene oxidation. However, co-precipitated catalysts gave somewhat different results, as expected, because of the bulk mixed oxide phases that were formed by this synthesis method, which did not optimize the formation of the vanadium oxide monolayer. More recent studies by Gasior et al.[167,169] demonstrate that even physical mixtures of crystalline V_2O_5 and TiO_2 (anatase) can form vanadium oxide monolayer catalysts that are effective for o-xylene oxidation by thermal spreading of V_2O_5 over the TiO_2 support. The thermal spreading of vanadium oxide over TiO_2 explains why the preparation method cannot influence the structure or reactivity of vanadium oxide monolayer catalysts after the catalysts are equilibrated.[138]

The role of the specific structure of the titania support (anatase and rutile) in the oxidation of o-xylene has also been greatly discussed in the literature.[168,170] Vejux and Courtine[170] claimed that the anatase structure of titania is a superior catalyst than the rutile structure of titania because of the close structural match between crystalline V_2O_5 and TiO_2 (anatase). However, these conclusions were not confirmed by subsequent investigators, who found no significant differences between the anatase and rutile modifications of titania supports upon the properties of the vanadium oxide monolayers.[78,168] In light of our current understanding of vanadium oxide monolayer catalysts, it is clear that the model proposed by Vejux and Courtine[170] is incorrect since the active vanadium oxide in these catalysts is not the crystalline V_2O_5 phase, but the two-dimensional vanadium oxide overlayer. Furthermore, the physical and chemical nature of the two-dimensional vanadium oxide overlayer is identical on both anatase and rutile modifications of titania.[171] The reactivity differences between anatase and rutile modifications of titania reported by Vejux and Courtine[170] were undoubtedly due to the presence of impurities in the pigment grade titania used in these early experiments, which have subsequently been reported by others.[119,135] It is now generally agreed that the modification of the titania support is not critical for the catalytic performance of vanadium oxide monolayer catalysts.

E. Selective Catalytic Reduction of NO_x (DeNOx)

The selective catalytic reduction (SCR) of NO_x with ammonia is currently of great interest because of the desire to minimize pollution from stationary emissions related to acid rain formation. Reactivity trends of the surface vanadium oxide species as a function of oxide support were also determined for the SCR of NO_x: $V_2O_5/TiO_2 > V_2O_5/ZrO_2 > V_2O_5/Al_2O_3 > V_2O_5/SiO_2$.[155] Corresponding TPR studies revealed that the activity of the supported vanadium oxide catalysts correlate with ease of reducibility of the surface vanadium oxide phase. It is thus not surprising that the selective catalytic reduction of NO_x is industrially conducted with the very active vanadium oxide monolayer catalysts on a titania support.[172] The TOFs for this

reaction vary by less than one order of magnitude with the oxide support, which possibly reflects that the DeNOx reaction is a bimolecular reaction involving the interaction of two molecules with the active surface sites, whereas most of the prior reactions discussed, especially methanol oxidation, occur via a unimolecular reaction involving the interaction of a single reactant molecule with the surface vanadium oxide sites.

Several studies have reported that the reactivity of the surface vanadium oxide species for the DeNOx reaction is sensitive to surface vanadium oxide coverage and the TOF increases approximately an order of magnitude with increasing surface coverage.[173,174] Increasing the surface vanadium oxide coverage simultaneously affects the number of surface hydroxyls,[70] the number of surface Bronsted acid sites,[48,70] the ~930 cm^{-1} Raman band assigned to a polymerized surface vanadium oxide species[173] and the number of nearest neighbors in the overlayer (surface crowding).[175] The methanol oxidation TOF over V_2O_5/TiO_2 does not exhibit a coverage dependence that shows that the redox properties do not depend on coverage and that methanol oxidation is also a structure insensitive reaction. The differences between methanol oxidation and SCR of NO_x as a function of surface vanadium oxide coverage reveal that the $DeNO_x$ reaction is a structure sensitive reaction that is influenced by its immediate environment (see later under Effect of Additives on Reactivity). Current studies are addressing the relative concentrations of the above factors to the surface coverage dependence of the SCR of NO_x reaction over supported vanadium oxide catalysts.[176] Preliminary findings reveal that the structure sensitive SCR of NO_x is influenced by the immediate environment, nearest surface metal oxide neighbors and surface Bronsted acid sites, of the surface vanadium oxide species.

Critical in the study of the SCR of NO with NH_3 is determining the mechanism by which the reaction occurs. Various reaction pathways have been proposed that essentially follow the Langmuir-Hinshelwood[177,178] or the Eley-Rideal[179–181] mechanisms. The Langmuir-Hinshelwood reaction can be written as follows:

$$NO^{gas} \rightarrow NO^{ads} \quad (1)$$

$$NH_3^{gas} \rightarrow NH_x^{ads} \quad (2)$$

$$NO^{ads} + NH_x^{ads} \rightarrow N_2^{gas} + H_2O^{gas} \quad (3),$$

and the Eley-Rideal mechanism can be written as:

$$NH_3^{gas} \rightarrow NH_x^{ads} \quad (4)$$

$$NO^{gas} + NH_x^{ads} \rightarrow N_2^{gas} + H_2O^{gas} \quad (5).$$

The differences in the proposed mechanism for SCR of NO have been ascribed to the differences in reaction conditions.[172] Under dilute conditions, the Eiley-Rideal mechanism is thought to occur since no chemisorbed NO species is detected by *in situ* FT-IR spectroscopy, and these reaction conditions are more relevant to industrial situations. Dumesic et al.[182] recently observed a modified Eiley-Rideal

mechanism to be the best suited for fitting the experimentally observed reaction rate. Svachula et al.[183] and Robinson et al.[184] have used a modified Eiley-Rideal mechanism to describe the SCR of NO over commercial catalysts based on vanadium oxide with some success.

F. Partial Oxidation of Methane by Molecular Oxygen

The partial oxidation of methane to methanol and formaldehyde over a suitable catalyst has attracted much attention. Many catalysts have been studied for this process and the V_2O_5/SiO_2 catalyst was found to be the most effective (active and selective) catalysts for the partial oxidation of methane to formaldehyde using N_2O and molecular oxygen as oxidants.[185–187] To study the effect of support, several supported vanadium oxide catalysts (V_2O_5/SiO_2, V_2O_5/TiO_2, and V_2O_5/SnO_2) were studied.[188] This study revealed that the V_2O_5/SiO_2 was the most selective catalyst for formaldehyde formation, whereas only the deep oxidation products ($CO+CO_2$) were produced over the V_2O_5/TiO_2 and V_2O_5/SnO_2 catalysts. The trend in selectivity was related to the extent of oxidization of the surface vanadium oxide species during methane oxidation as observed by *in situ* Raman spectroscopy: V_2O_5/SiO_2 > V_2O_5/TiO_2 > V_2O_5/SnO_2. The more reducible catalysts were found to more extensively oxidize CH_4 toward CO_2. The trend in activity for methane oxidation was: V_2O_5/SnO_2 > V_2O_5/TiO_2 > V_2O_5/SiO_2. The lower activity of the V_2O_5/TiO_2 catalyst for CH_4 oxidation is somewhat surprising and may reflect the unusual demands of this high temperature reaction. The influence of surface vanadium oxide coverage on the methane oxidation activity was also examined, and the TOF was found to be independent of vanadium oxide loading (0.25–5% V_2O_5/SiO_2). This suggests that CH_4 oxidation is a structure insensitive reaction requiring only an isolated surface vanadium oxide species.

G. Dependence of Turnover Frequency for Different Reactions

The turnover frequencies for the oxidation of different molecules over monolayer V_2O_5/TiO_2 catalysts, approximately 12 μmole V^{5+}/m^2, are compared in Table 11. The data were collected from various oxidation studies reported in the literature. Such a comparative study among different research groups can now be performed since we know that the different preparation methods do not affect the molecular structures of the surface vanadium oxide species,[138] and we assume that the catalysts used are relatively uncontaminated. The TOFs are listed as total oxidation TOF (reflects the oxidation of reactant molecules) and as partial oxidation TOF (reflects the selective oxidation of reactant molecules to partial oxidation products).

Examination of Table 11 reveals that the TOF for the oxidation of methanol is very high relative to the TOFs for the oxidation of hydrocarbons. This difference in TOFs reflects the different types of rate determining steps occurring during these

TABLE 11
TOF for Different Oxidation Reactions over Monolayer V_2O_5/TiO_2 Catalysts

Reaction	Ref	Temp (°C)	TOF (s^{-1})	TOF[a] (s^{-1})	Effect of θ[b] (for $\theta \leq 0.75$)
CH_3OH	TW	230	1.1	1.1	no
CO	114	[c]	$2*10^{-2}$	$2*10^{-2}$	yes
Buta-1,3-diene (C_4H_6)	189	389	$2.8*10^{-2}$	$1.1*10^{-2}$ ($C_4H_2O_3+C_4H_4O$)	yes
But-1-ene (C_4H_8)	189	389	$2.3*10^{-3}$	$7.4*10^{-3}$ ($C_4H_2O_3$)	no
Furan (C_4H_4O)	190	389	$1.8*10^{-2}$	$8.6*10^{-3}$ ($C_4H_2O_3$)	no
Benzene (C_6H_6)	191	389	$3.2*10^{-2}$	$2.9*10^{-3}$ ($C_4H_2O_3$)	yes
Toluene	121	380	$2.2*10^{-2}$	$1.3*10^{-2}$ (BA+BzA)	ND
o-Xylene	192	389[d]	$1.0*10^{-2}$	$8*10^{-3}$ (PA)	yes
$NO+NH_3$	114	227[d]	$3.0*10^{-3}$	$3.0*10^{-3}$	no (for $\theta>0.3$)
$NO+NH_3$	173	227	$4.0*10^{-3}$	$4.0*10^{-3}$	yes (small for $\theta>0.21$)
$NO+NH_3$	174	227	$5.3*10^{-3}$	$5.3*10^{-3}$	yes (small for $\theta>0.25$)

[a] Represents turnover frequency for partial oxidation products(s) noted in parenthesis: BA-benzaldehyde, BzA-benzoic acid, PA-phthalic anhydride.
[b] θ = surface coverage.
[c] Temperature of reaction not mentioned in reference.
[d] Extrapolated using activation energies of 32 kcal/mole and 12 kcal/mole for o-xylene and $NO+NH_3$, respectively.
TW = this work.
ND = not determined.

reactions. The rate-determining step during methanol oxidation is the cleavage of the C-H bond of the surface methoxy intermediate (see the first section in part V). The oxidation of hydrocarbons involves both cleavage of C-H bonds and insertion of oxygen.[140] The much lower TOF for the oxidation of hydrocarbons is apparently a consequence of the slow oxygen insertion step. This is supported by the low TOF exhibited by the CO oxidation reaction where only an oxygen insertion step is required and hydrogen abstraction cannot occur. Furthermore, the methanol oxidation TOF is not a function of surface vanadium oxide coverage, whereas the oxidation TOFs for CO and the hydrocarbons appear to possess a dependence on the surface vanadium oxide coverage. The selective catalytic reduction of NO by NH_3 also exhibits a very low TOF and is a function of surface vanadium oxide coverage. This behavior also may be due to the presence of an oxygen insertion rate-determining step, but the bimolecular nature of this reaction provides addi-

tional variables. In summary, the oxidation TOF is a strong function of the specific molecule to be oxidized and reactions that involve oxygen insertion rate-determining steps appear to be slower than reactions that involve C-H bond cleavage rate determining steps.

H. Effect of Additives on Reactivity

The effect of promoters/impurities on the 1% V_2O_5/TiO_2 catalyst was studied for the methanol oxidation reaction, and the results are shown in Table 12. It was noted in part IV that the dehydrated Raman studies revealed that tungsten, niobium, and silicon oxides essentially did not interact with the surface vanadium oxide species and that potassium and phosphorous oxides interacted with and altered the surface vanadium oxide species. Examination of Table 12 reveals that the noninteracting promoters (tungsten oxide, niobium oxide, and silica) do not affect the activity or selectivity of the 1% V_2O_5/TiO_2 catalyst. However, the interacting promoters (potassium oxide and phosphorous oxide) significantly reduced the TOF of the 1% V_2O_5/TiO_2 catalyst. Thus promoters that preferentially coordinate to the oxide support via reaction with the surface hydroxyls (tungsten oxide, niobium oxide, and silica) do not affect the structure or reactivity of the surface vanadium oxide species for methanol oxidation. However, promoters that preferentially coordinate with the surface vanadia site (phosphorous and potassium) influence the structure and reactivity of the surface vanadium oxide species for methanol oxidation.

The influence of some of the above promoters/additives on the performance of a 1% V_2O_5/TiO_2 catalyst for the SCR of NO_x was also examined.[176] The exact same catalysts that were examined above for methanol oxidation were used in the DeNOx studies. The influence of the promoters/additives upon the SCR of NO_X was very different than that found for the oxidation of methanol. The addition of

TABLE 12
Methanol Oxidation Turnover Frequency for Promoters on 1%V_2O_5/TiO_2

Promoters on 1% V_2O_5/TiO_2	TOF to HCHO (sec^{-1})
None	2.0
6% Nb_2O_5	1.6
3% SiO_2	2.7
7% WO_3	3.4
0.3% K_2O	0.5
0.7% K_2O	0.07
5% P_2O_5	0.06

surface tungsten oxide and niobium oxide increased the SCR TOF by approximately an order of magnitude, whereas the same additives had no appreciable effect on methanol oxidation. This suggests that the redox activity of the tungsten/niobium oxide promoted 1% V_2O_5/TiO_2 catalyst was not perturbed by these additives, since the structure insensitive methanol oxidation probes this property, and that these additives are affecting the environment around the surface vanadium oxide species, which the bimolecular NO_x and NH_3 reaction is sensitive to (nearest number of surface metal oxide neighbors and Bronsted acid sites). Promoters that preferentially interact with the surface vanadia species (phosphorous and potassium) are known poisons for the SCR of NO_x reaction.[193] The methanol oxidation probe reaction showed that these promoters reduce the redox activity of the surface vanadia sites. Furthermore, potassium is also known to destroy the surface Bronsted acid sites in V_2O_5/TiO_2 catalysts.[194] Thus the same promoters have a different effect on simple unimolecular reactions such as methanol oxidation, which only require single redox (structure insensitive reaction) sites, and a bimolecular reaction such as NO_x and NH_3, which depends on the redox sites as well as their environments (structure-sensitive reaction).

VI. CONCLUSIONS

Rather impressive advances have been made in the last few years regarding our fundamental understanding of supported vanadium oxide catalysts. The characterization methods now available to determine the molecular structures of the surface metal oxide phases (especially Raman spectroscopy and solid-state ^{51}V NMR, and to lesser extents IR and EXAFS/XANES) have been critical in establishing a sound fundamental foundation. These studies have revealed that under ambient conditions, the surface vanadium oxide molecular structures are directly related to the net surface pH at PZC of the thin aqueous film on the oxide supports and can be predicted from the corresponding aqueous chemistry. Under *in situ* conditions, the dehydrated surface vanadium oxide species shows two types of behavior. The first type of surface vanadium oxide behavior is present on SiO_2 where an isolated, three-legged $(SiO)_3V{=}O$ species exists at all vanadium oxide loadings. The second type of surface vanadium oxide behavior exists on Al_2O_3, TiO_2, ZrO_2, and Nb_2O_5. Essentially the same dehydrated surface vanadium oxide structures are present on these oxide supports as well as on different oxide support structures (anatase, rutile, brookite, or B-phase). The preparation method also does not influence the surface vanadium oxide structure because the surface vanadia species spontaneously disperse in equilibrated catalysts. The assignments of the broad *in situ* Raman bands at ~900 cm^{-1}, however, are still not fully understood at present, and additional studies need to be performed to conclusively assign these *in situ* Raman bands. Additional structural information about reduced surface vanadium oxide sites is also needed from EPR and EXAFS/XANES studies.

The reactivity studies revealed that the specific oxide support controls the activity of the surface vanadium oxide species and is independent of surface vanadium oxide coverage for unimolecular reactions. The more reducible oxide supports, such as titania and zirconia, result in more active catalysts and the less reducible oxide supports, such as silica and alumina, result in significantly less active catalysts. The reducibility controls the reactivity of the supported vanadium oxide catalysts by controlling the number of active sites and/or activity per site. The specific structure of the oxide support (anatase, rutile, brookite, B-phase), however, does not influence the reactivity of the surface vanadium oxide species. The influence of the support is believed to occur via the V-O-S bond where the support acts as a ligand that controls the redox properties of the surface vanadium oxide overlayer. The pronounced influence of the oxide support upon vanadium oxide monolayer catalysts has been demonstrated for numerous reactions and is a general phenomenon.

For reactions involving large molecules or two molecules, the immediate environment around the surface vanadium oxide sites may also be important and such reactions may show nonlinear behavior with surface vanadium oxide coverage (e.g., DeNO$_x$, o-xylene). For simple unimolecular reactions (structure insensitive reactions), promoters that preferentially interact with the oxide support (tungsten oxide, niobium oxide, silica) do not alter the reactivity of the surface vanadium oxide species, and only promoters that directly interact with the surface vanadium oxide species (alkali, phosphorous, etc.) affect the reactivity of the surface vanadium oxide species. For reactions involving large molecules or two molecules (structure-sensitive reactions), all promoters influence the reactivity of supported vanadium oxide catalysts since they change the environment around the active surface vanadium oxide species. Thus the reactivity of a given supported vanadium oxide catalyst also depends on the specific requirements of the reaction. Very little is still understood about the characteristics that control reaction selectivity, and future investigations will need to address this very important issue.

ACKNOWLEDGMENTS

Financial support of NSF Program No. INT-8822945 and the Polish Academy of Sciences for this international cooperative science program is gratefully acknowledged.

REFERENCES

1. **Bond, G. C.; Tahir, S. F.,** *Appl. Catal.*, 1991, *71*, 1.
2. **Gellings, P. J.,** *Specialist Periodical Reports - Catalysis*, G. C. Bond, G. Webb, Eds., Royal Society of Chemistry, London, 1985, *7*, 105.
3. **Hucknall, D. J.,** *Selective Oxidation of Hydrocarbons*, Academic Press, London, 1974.
4. **Villadsen, J.; Livbjerg, H.,** *Catal. Rev. Sci. Eng.*, 1978, *17*, 203.

5. **Wainwright, M. S.; Foster, N. R.,** *Catal. Rev. Sci. Eng.,* 1979, *19*, 211.
6. **Bielanski, A; Haber, J.,** *Catal. Rev. Sci. Eng.,* 1979, *19*, 1.
7. **Dadyburjor, D. B.; Jewur, S. S.; Ruckenstein, E.,** *Catal. Rev. Sci. Eng.,* 1979, *19*, 293.
8. **Baes, C. F., Jr.; Mesmer, R. E.,** *The Hydrolysis of Cations*, Wiley, New York, 1970.
9. **Trotter, J.; Barnes, W. H.,** *Can. Mineral*, 1958, *7*, 161.
10. **Sleight, A. W.; Chen, H. Y.; Ferretti, A.; Cox, D. E.,** *Mater. Res. Bull.,* 1979, *14*, 1571.
11. **Tillmanns, E.; Baurs, W. H.,** *Acta Crystallogr.,* 1971, B27, 2124.
12. **Gopal, R.; Calvo, C.,** *Can. J. Chem.,* 1971, *49*, 3056.
13. **Au, P. K. L.; Calvo, C.,** *Can. J. Chem.,* 1967, *45*, 2297.
14. **Gopal, R.; Calvo, C.,** *Can. J. Chem.,* 1973, *51*, 1004.
15. **Gopal, R.; Calvo, C.,** *Acta Crystallogr.,* 1974, *B30*, 2491.
16. **Evans, H. T., Jr.,** *Z. Kristallogr.,* 1960, *114*, 257.
17. **Marumo, F.; Isobe, M.; Iwai, S.,** *Acta Crystallogr.,* 1974, *B30*, 1628.
18. **Baran, E. J.; Botto, I. L.,** *Monatshefte für Chemie*, 1977, *108*, 311.
19. **Jordan, B. D.; Calvo, C.,** *Can. J. Chem.,* 1974, *52*, 2701.
20. **Bachmann, H. G.; Ahmed, F. R.; Barnes, W. H.,** *Z. Kristallogr., Kristallgeom., Kristallchem.,* 1961, *115*, 110.
21. **Durif, A.; Averbuch-Pouchot, M. T.; Guitel, J. C.,** *Acta Crystallogr.,* 1980, *B36*, 680.
22. **Haber, J.,** in *Structure and Reactivity of Surfaces*; C. Morterra, A. Zecchina, G. Costa, Eds., Stud. Surf. Sci. Catal., Elsevier, 1989, *48*, 447.
23. **Griffith, W. P.; Wickins, T. D.,** *J. Chem. Soc.* (A), 1966, 1087.
24. **Griffith, W. P.,** *J. Chem. Soc.* (A), 1967, 905.
25. **Griffith, W. P.; Lesnaik, P. J. B.,** *J. Chem. Soc.* (A), 1969, 1066.
26. **Brown, R. G.; Ross, S. D.,** *Spectroshimica Acta*, 1972, *28A*, 1263.
27. **Botto, I. L.; Baran, E. J.; Pedregosa, J. C.; Aymonino, P. J.,** *Monatshefte für Chemie*, 1979, *110*, 895.
28. **Onodera, S.; Ikegami, Y.,** *Inorg. Chem.,* 1980, *19(3)*, 615.
29. **Deo, G.; Hardcastle, F. D.; Richards, M.; Wachs, I. E.; Hirt, A. M.,** in *Novel Materials in Heterogeneous Catalysis*, Baker, R.T.K., Murrell, L. L., Eds., ACS Symposium Series 437, American Chemical Society: Washington, DC, 1990, 317.
30. **Deo, G.; Hardcastle, F. D.; Richards, M.; Wachs, I. E.; Hirt, A. M.,** *Prepr.-Am. Chem. Soc., Div. Pet. Chem.,* 1989, *34(3)*, 529.
31. **Hardcastle, F. D.; Wachs, I. E.,** *J. Phys. Chem.,* 1991, *95*, 5031.
32. **Roozeboom, F; Fransen, T.; Mars, P.; Gellings, P. J.,** *Z. Anorg. Allg. Chem.,* 1979, *449*, 25.
33. **Roozeboom, F.; Mittelmeijer-Hazeleger, M. C.; Moulijn, J. A.; Medema, J.; de Beer, V. H. J.; Gellings, P. J.,** *J. Phys. Chem.,* 1980, *84*, 2783.
34. **L. Wang,** in *Preparation and Characterization of Molybdenum-Alumina and Related Catalyst Systems*, Ph.D. dissertation, University of Wisconsin, Milwaukee, University Microfilms International, Ann Arbor, MI, 1982.
35. **Chan, S. S.; Wachs, I. E.; Murell, L. L.; Wang, L.; Hall, W. K.,** *J. Phys. Chem.,* 1984, *88*, 5831.
36. **Wachs, I. E.; Chan, S. S.; Chersich, C. C.; Saleh, R. Y.,** in *Catalysis on the Energy Scene*, Studied in Surface Science, S. Kaliaguine, A. Mahay, Eds., Elsevier, Amsterdam, 1984, *19*, 275.
37. **Saleh, R. Y.; Wachs, I. E.; Chan, S. S.; Chersich, C. C.,** *J. Catal.,* 1986, *98*, 102.
38. **Wachs, I. E.; Hardcastle, F. D.,** in *Proc. 9th Inter. Congr. Catal., Calgary*; M. J. Phillips and M. Ternan, Eds., 1988, *3*, 1449.
39. **Wachs, I. E.; Hardcastle, F. D.; Chan, S. S.,** *Mat. Res. Soc. Symp. Proc.,* 1988, *111*, 353.
40. **Le Coustumer, L. R.; Taouk, B.; Le Meur, M.; Payen, E.; Guelton, M.; Grimblot, J.,** *J. Phys. Chem.,* 1988, *92*, 1230.
41. **Hausinger, G.; Schmelz, H.; Knözinger, H.,** *Appl. Catal.,* 1988, *39*, 267.
42. **Cristiani, C.; Forzatti, P.; Busca, G.,** *J. Catal.,* 1989, *116*, 586.

43. **Wokaun, A.; Schraml, M.; Baiker, A.,** *J. Catal.,* 1989, *116*, 595.
44. **Wachs, I. E.; Jehng, J.-M.; Hardcastle, F. D.,** *Solid State Ionics,* 1989, *32/33*, 904.
45. **Oyama, S. T.; Went, G. T.; Lewis, K. B.; Bell, A. T.; Somarjai, G.A.,** *J. Phys. Chem.,* 1989, *93*, 6786.
46. **Ramis, G.; Cristiani, C.; Forzatti, P.; Busca, G.,** *J. Catal.,* 1990, *124*, 574.
47. **Went, G.; Oyama, S. T.; Bell, A. T.,** *J. Phys. Chem.,* 1990, *94*, 4240.
48. **Hatayama, F.; Ohna, T.; Maruoka, T.; Ono, T.; Miyata, H.,** *J. Chem. Soc. Faraday Trans.,* 1991, *87*, 2629.
49. **Deo, G.; Wachs, I. E.,** *J. Phys. Chem.,* 1991, *95*, 5889.
50. **Deo, G.; Wachs, I. E.,** *J. Catal.,* 1991, *129*, 307.
51. **Vuurman, M. A.; Hirt, A. M.; Wachs, I. E.,** *J. Phys. Chem.,* 1991, *95*, 9928.
52. **Went, G.; Leu, L.-J.; Lombardo, S. J.; Bell, A.T.,** *J. Phys. Chem.,* 1992, *96*, 2235.
53. **Vuurman, M.A.; Wachs, I.E.,** *J. Phys. Chem.,* 1992, *96*, 5008.
54. **Scharf, U.; Schraml-Marth, M.; Wokaun, A.; Balker, A.,** *J. Chem. Soc. Faraday Trans.,* 1991, *87*, 3299.
55. **Wachs, I. E.; Deo, G.; Kim, D. S.; Vuurman M. A.; Hu, H.,** in *New Frontiers in Catalysis,* Proc. 10th Inter. Congr. Catal., Budapest, 1992, Vol. A, 543.
56. **Hardcastle, F. D.; Wachs, I. E.,** *Catalysis,* Royal Society of Chemistry, 1993, 10, 102.
57. **Frederickson, L. D.; Hausen, D. M.,** *Anal. Chem.,*1963, *35*, 818.
58. **Vuurman, M. A.,** in *Spectroscopic Characterization of Supported Metal Oxide Catalysts,* Ph.D dissertation, University of Amsterdam, Netherlands, 1992.
59. **Busca, G.,** *Mater. Chem. Phys.,* 1988, *19*, 157.
60. **Miyata, H.; Kohno, M.; Ono, T.; Ohno, T.; Hatayama, F.,** *J. Mol. Catal.,* 1990, *63*, 181.
61. **Busca, G.; Elmi, A. S.; Forzatti, P.,** *J. Phys. Chem.,* 1987, *91*, 5263.
62. **Busca, G.,** *J. Mol. Catal.,* 1989, *50*, 241.
63. **Elmi, A. S.; Tronconi, E.; Cristiani, C.; Martin, J. P. G.; Forzatti, P.; Busca, G.,** *Ind. Eng. Chem. Res.,* 1989, *28*, 387.
64. **Escribano, V. S.; Busca, G.; Lorenzelli, V.,** *J. Phys. Chem.,* 1990, *94*, 8939.
65. **Escribano, V. S.; Bitsca, G.; Lorenzelli, V.,** *J. Phys. Chem.,* 1990, *94*, 8945.
66. **Escribano, V. S.; Busca, G.; Lorenzelli, V.,** *J. Phys. Chem.,* 1991, *95*, 5541.
67. **Busca, G.,** *Prepr.-Am. Chem. Soc., Div. Pet. Chem.,* 1992, *37(4)*, 1054.
68. **Miyata, H.; Nakagawa, Y.; Ono, T.; Kubokawa, Y.,** *Chem. Letters,* 1983, 1141.
69. **Miyata, H.; Fujii, K.; Ono, T.,** *J. Chem. Soc. Faraday Trans.,* 1988, *84*, 3121.
70. **Turek, A. M.; DeCanio, E.; Wachs, I. E.,** *J. Phys. Chem.,* 1992, *96*, 5000.
71. **Little, L.H.,** *Infrared Spectra of Absorbed Species,* London, Academic Press, 1966.
72. **C. R. Brundle, C. A. Evans, Jr., S. Wilson,** Eds., *Encyclopedia of Materials Characterization,* Butterworth-Heinemann, Stoneham, 1992.
73. **Eckert, H.; Wachs, I. E.,** *Mater. Res. Soc. Symp. Proc.,* 1988, *111*, 455.
74. **Eckert, H.; Wachs, I. E.,** *J. Phys. Chem.,* 1989, *93*, 6796.
75. **Lapina, O. B.; Mastikhin, V. M.; Shubin, A. A.; Krasiln, V. N.; Zamareev, K. I.,** *Progress in NMR Spectroscopy,* 1992, *24*, 457.
76. **Lapina, O. B.; Mastikhin, V. M.; Simonova, L. G.; Bulgakova, Yu. 0.,** *J. Mol. Catal.,* 1991, *69*, 61.
77. **Sobalik, Z.; Markvart, M.; Stopka, P.; Lapina, O. B.; Mastikhin, V. M.,** *J. Mol. Catal.,* 1992, *71*, 69.
78. **Inomata, M.; Mori, K.; Miyamoto, A.; Ui, T.; Murakami, Y.,** *J. Phys. Chem.,* 1983, *87*, 754.
79. **Centi, G.; Giamello, E.; Pinelli, D.; Trifiro, F.,** *J. Catal.,* 1991, *130*, 220.
80. **Centi, G.; Pinelli, D.; Trifiro, F.; Ghoussoub, D.; Guelton, M.; and Gengembre, L.,** *J. Catal.,* 1991, *130*, 238.
81. **Kozlowski, R.; Pettifer, R.F.; Thomas, J. M.,** *J. Phys. Chem.,* 1983, *87*, 5176.
82. **Haber, J.; Kozlowska, A.; Kozlowski, R.,** *J. Catal.,* 1986, 102, 52.
83. **Tanaka, T.; Yamashita, H.; Tsuchitani, R.; Funabiki, T.; Yoshida, S.,** *J. Chem. Soc., Faraday Trans. 1.,* 1988, *84*, 2987.

84. **Yoshida, S.; Tanaka, T.; Nishimura, Y.; Mizutani, H.,** in *Proc. 9th Inter. Congr. Catal.*, M. J. Phillips and M. Ternan, Eds., Calgary, 1988, *3*, 1473.
85. **Yoshida, S.; Tanaka, T.; Hanada, T.; Hiraiwa, T.; Kanai, H.,** *Catal. Lett.*, 1992, *12*, 277.
86. **Bond, G. C.; Flamerz, S.,** *Appl. Catal.*, 1989, *46*, 89.
87. **Kerkhof, F. P. J. M.; Moulijn, J. A.,** *J. Phys. Chem.*, 1979, *83*, 1612.
88. **Busca, G.; Giamello, E.,** *Materials Chemistry and Physics*, 1990, *25*, 475.
89. **Brant, P.; Saleh, R. Y.; Wachs, I. E.,** unpublished results.
90. **Dryek, K.; Serwicka, E.; Grzybowska, B.,** *React. Kinet. Catal. Lett.*, 1979, *10*, 93.
91. **Fierro, F. L. G.; Gambaro, L. A.; Gonzalez-Elipe, A. R.; Soria, J.,** *Colloids Surf.*, 1984, *11*, 31.
92. **Busca, G.; Marchetti, L.; Centi, G.; Trifiro, F.,** *J. Chem. Soc. Faraday Trans., 1*, 1985, *81*, 1003.
93. **Busca, G.; Centi, G.; Marchetti, L.; Trifiro, F.,** *Langmuir*, 1986, *2*, 568.
94. **Anpo, M.; Sunamoto, M.; Che, M.,** *J. Phys. Chem.*, 1989, *93*, 1187.
95. **Iwamoto, M.; Furukawa, H.; Matsukami, K.; Takenaka, T.; Kagawa, S.,** *J. Am. Chem. Soc.*, 1983, *105*, 3719.
96. **Hazenkamp, M. F.; Blasse, G.,** *J. Phys. Chem.*, 1992, *96*, 3442.
97. **Fournier, M.; Louis, C.; Che, M.; Chaquin, P.; Masure, D.,** *J. Catal.*, 1989, *119*, 400.
98. **Masure, D.; Chaquin, P.; Louis, C.; Che, M.; Fournier, M.,** *J. Catal.*, 1989, *119*, 400, 415.
99. **Weckhuysen, B. M; Leeman, H.; Schoonheydt, R. A; Deo, G.; Wachs, I. E.,** unpublished results.
100. **Jones, A.; McNicol, B. D.,** *Temperature Programmed Reduction For Solid Material Characterization,* Marcel Dekker, New York, 1986.
101. **Roozeboom, F.; van Dillen, A. J.; Geus, J. W.; Gellings, P. J.,** *Ind. Eng. Chem. Prod. Res. Dev.*, 1981, *20*, 304.
102. **Roozeboom, F.; Cordingley, P. D.; Gellings, P. J.,** *J. Catal.*, 1981, *68*, 464.
103. **Bond, G. C.; Zurita, J. P.; Flamerz, S.; Gellings, P. J.; Bosch, H.; van Ommen, J. G.; Kip, B. J.,** *Appl. Catal.*, 1986, *22*, 361.
104. **Koranne, M. M.; Goodwin, J. G.; Marcelin, G.,** Paper# 49e, AIChE 1992, Miami.
105. **Reddy, N. K.; Chary, K. V. R.; Reddy, B. M.; Rao, B. R.; Subramanium, V. S.,** *Appl. Catal.*, 1984, *9*, 225.
106. **Nag, N. K.; Chary, K. V. R.; Rao, B. R.; Subramanyum, V. S.,** *Appl. Catal.*, 1987, *31*, 73.
107. **Chary, K. V. R.,** *J. Chem. Soc., Chem. Commun.*, 1989, 104.
108. **Chary, K. V. R.; Narsimha, K.; Rao, K. S. R.; Rao, B. R.; Rao, P. K.,** *J. Mol. Catal.*, 1990, *58*, L13.
109. **Chary, K. V. R.; Rao, B. R.; Subrahmanyam, V. S.,** *Appl. Catal.*, 1991, *74*, 1.
110. **Reddy, B. M.,** *Prepr.-Am. Chem. Soc., Div. Pet. Chem.*, 1992, *37(4)*, 1251.
111. **Niwa, M.; Inagaki, S.; Murakami, Y.,** *J. Phys. Chem.*, 1985, *89*, 3869.
112. **Niwa, M.; Matsuoka, Y.; Murakami, Y.,** *J. Phys. Chem.*, 1989, *93*, 3660.
113. **Eberhardt, M. A.; Houalla, M.; Mulcahy, F. M.; Hercules, D.M.,** paper # B03, 13th North American Meeting Catalysis Society, Pittsburgh, 1993.
114. **Murakami, Y.; Inomata, M.; Miyamoto, A.; Mori, K.,** in *Proc. 7th Intl. Congr. Catal.*, T. Seiyama and K. Tanabe, Eds., Tokyo, 1980, *B*, 1344.
115. **Miyamoto, A.; Yamazaki, Y.; Inomata, M.; Murakami, Y.,** *J. Phys. Chem.*, 1981, *85*, 2366.
116. **Cavani, F.; Foresti, E.; Parrinello, F.; Trifiro, F.,** *Appl. Catal.*, 1988, *38*, 311.
117. **Centi, G.; Pinelli, D.; Trifiro, F.,** *J. Mol. Catal.*, 1990, *59*, 221.
118. **Brazdil, J.,** in *Characterization of Catalytic Materials*, I. E. Wachs, Ed., Butterworth-Heinemann, Stoneham, 1992.
119a. **van Hengstum, A. J.; van Ommen, J. G.; Bosch, H.; Gellings, P. J.,** in *Proc. 8th Inter. Congr. Catal.*, Berlin, 1984, *4*, 297.
119b. **van Hengstum, A. J.; Pranger, J.; van Ommen, J.G.; Gellings, P. J.,** *Appl. Catal.*, 1984, *11*, 317.
120. **Zhu, J.; Anderson, S. L. T.,** *Appl. Catal.*, 1989, *53*, 251.

121. **Zhu, J.; Anderson, S. L. T.,** *J. Chem. Soc., Faraday Trans., 1,* 1989, *85,* 3629.
122. **Zhu, J.; Rebenstorf, B.; Anderson, S. L. T.,** *J. Chem. Soc., Faraday Trans., 1,* 1989, *85,* 3645.
123. **Deo, G.,** *Molecular Design of Supported Vanadium Oxide Catalysts,* Ph.D. dissertation, Lehigh University, 1992.
124. **Park, G. A.,** *Chem. Rev.,* 1965, *65,* 177.
125. **Gil-Llambias, F. J.; Escudey, A. M.; Fierro, J. L. G.; Lopez Agudo, A.,** *J. Catal.,* 1985, *95,* 520.
126. **Haber, J.; Marcezewski, A. W.; Sprycha, R.; Szczypa, J.,** Proc. 2nd International Symposium on Surface Charge Characterization, San Jose, CA, 1991.
127. **Kohler, S. D.; Ekerdt, J. G.; Kim, D. S.; Wachs, I. E.,** *Catal. Lett.,* 1992, *16,* 231.
128. **Roark, R. D.; Kohler, S. D.; Ekerdt, J. G.; Kim, D. S.; Wachs, I. E.,** *Catal. Lett.,* 1992, *16,* 77.
129. **Mastikhin, V. M.; Mudrakovsky, I. L.; Nosov, A. V.,** Progress in NMR Spectroscopy, 1991, *23,* 259.
130. **Segawa, K.; Hall, W. K.,** *J. Catal.,* 1982, *77,* 221.
131. **Kim, D. S.; Kurusu, Y.; Segawa, I.; Wachs, I. E.,** in *Proc. 9th Inter. Congr. Catal.,* M. S. Phillips and M. Ternan, Eds., Chemical Institute Canada, Ontario, 1988, *4,* 1460.
132. **Das, N.; Eckert, H.; Hu, H.; Wachs, I. E.; Walzer, J.; Feher, F.,** *J. Phys. Chem.,* 1993, *97,* 8240.
133. **Das, N.; Eckert, H.; Deo, G.; Wachs, I. E.,** unpublished results.
134. **Bond, G. C.; Bruckman, K.,** Faraday Discuss. Chem. Soc., 1981, *72,* 235.
135. **van Hengstum, A. J.; van Ommen, J. G.; Bosch, H.; Gellings, P. J.,** *Appl. Catal.,* 1983, *8,* 369.
136. **Wachs, I. E.; Saleh, R. Y.; Chan, S. S.; Chersich, C. C.,** *Appl. Catal.,* 1985, *15,* 339.
137. **Haber, J.; Machej, T.; Czeppe, T.,** *Surf. Sci.,* 1985, 151, 301.
138. **Machej, T.; Haber, J.; Turek, A. M.; Wachs, I. E.,** *Appl. Catal.,* 1991, *70,* 115.
139. **Deo, G.; Wachs, I. E.,** *J. Catal.,* 1994, *146,* 323.
140. **Haber, J.,** in *Surface Properties and Catalysis by Non-Metals,* J. Bonnelle, B. Delmon, and E. Derouane, Eds., Reidel, Dordrecht, 1983, *1.*
141. **Haber, J.,** *Pure Appl. Chem.,* 1984, *56,* 1663.
142. **Haber, J.; Machej, T.; Czeppe, T.,** *Surface Sci.,* 1985, *151,* 301.
143. **Xie, Y. C.; Tang, Y. Q.,** *Adv. Catal.,* 1990, *37,* 301.
144. **Knozinger, H.; Taglauer, E.,** Specialist Periodical Report, Catalysis, vol. 10, Royal Society of Chemistry, London, 1993, 1.
145. **Deo, G.; Wachs, I. E.,** *J. Catal.,* 1994, *146,* 335.
146. **Jehng, J-M.; Deo, G.; Wachs, I. E.,** (to be published).
147. **Tatibouet, J.-M.; Germain, J. E.,** *J. Catal.,* 1981, *72,* 375.
148. **Tatibouet, J.-M.; Germain, J. E.,** *J. Catal.,* 1983, *82,* 240.
149. **Louis, C.; Tatibouet, J.-M.; Che, M.,** *J. Catal.,* 1988, *109,* 354.
150. **Kim, D. S.; Tatibouet, J.-M.; Wachs, I. E.,** *J. Catal.,* 1992, *136,* 209.
151. **Ohuchi, F.; Firment, L. E.; Chowdry, U.; Ferretti, A.,** *J. Vac. Sci. Technol.,* 1984, *A2,* 1022.
152. **Farneth, W. E.; Ohuchi, F.; Staley, R. H.; Chowdry, U.; Sleight, A. W.,** *J. Phys. Chem.,* 1985, *84,* 912.
153. **Yang, T. J.; Lunsford, J. H.,** *J. Catal.,* 1987, *103,* 55.
154. **Webber, R. S.,** *J. Phys. Chem.,* 1994, *98,* 2999.
155. **Nickl, J; Dutoit, D.; Baiker, A; Scharf, U.; Wokaun, A.,** *Ber Bunsenges. Phys. Chem.,* 1993, *97,* 217.
156. **Tauster, S. J.; Fung, S. C.; Baker, R. T. K.; Horsley, J. A.,** *Science,* 1981, *221,* 1121.
157. **Tauster, S. J.,** *Acc. Chem. Res.,* 1987, *20,* 389.
158. **Jehng, J.-M.; Wachs, I. E.,** *Catal. Lett.,* 1992, *13,* 9.
159. **Deo, G.; Haber, J.; Janas, J.; Wachs, I. E.,** unpublished results.
160. **Shikada, T.; Fujimoto, K.; Kunugi, T.; Tominaga, H.; Kanoko, S.; Kubo, Y.,** *Ind. Eng. Chem., Prod. Res. Dev.,* 1981, *20,* 91.
161. **Morikawa, S.; Yoshida, H.; Takahashi, K.; Kurita, S.,** *Chem. Lett.,* 1981, 251.

162. **Bjorkland, R. B.; Odenbrand, C. U. I; Brandan, J. G. M.; Anderson, L. A. H.; Liedberg, B.,** *J. Catal.,* 1989, *119*, 187.
163. **Grzybowska, B.; Haber, J.,** Eds., *Vanadia Catalysts for Processes of Oxidation of Aromatic Hydrocarbons*, Polish Scientific, Krakow, 1984.
164. **Grzybowska, B.,** in *Catalysis by Acids and Bases*, Studies in Surface Science and Catalysis, C. Naccache, G. Goudurier, Y. Boutaarit, J. C. Vedine, Eds., Elsevier, Amsterdam, 1985, 45.
165. **Hauffe, K.; Raveling, H.,** *Ber. Bunsenges, Phys. Chem.,* 1980, *84*, 912.
166. **Bond, G. C.; König, P.,** *J. Catal.,* 1982, *77*, 309.
167. **Gasior, M.; Gasior, I.; Grzybowska, B.,** *Appl. Catal.,* 1984, *10*, 87.
168. **Cavani, F.; Centi, G.; Foresti, E.; Trifiro, F.; Busca, G.,** *J. Chem. Soc., Faraday Trans., 1*, 1988, *84*, 237.
169. **Gasior, M.; Haber, J.; Machej, T.,** *Appl. Catal.,* 1987, *33*, 1.
170. **Vejux, A.; Courtine, P. J.,** *J. Solid State Chem.,* 1978, *23*, 93.
171. **Deo, G.; Turek, A. M.; Wachs, I. E.; Machej, T.; Haber, J.; Das, N.; Eckert, H.; Hirt, A. M.,** *Appl. Catal.,* 1992, *91*, 27.
172. **Bosch, H.; Janssen, F. J. J. G.,** *Catal. Today*, 1988, *2*, 369.
173. **Went, G.T.; Leu, L.-J.; Rosin, R.; Bell, A. T.,** *J. Catal.,* 1992, *134*, 492.
174. **Baiker, A.; Handy, B.; Nickl, J.; Schraml-Marth, M.; Wokaun, A.,** *Catal. Lett.,* 1992, *14*, 89.
175. **Szakacs, S.; Altena, G. J.; Fransen, T.; van Ommen, J. G.; Ross, J. R. H.,** *Catalysis Today,* 1992, *16*, 237.
176. **Deo, G.; Wachs, I. E.,** unpublished results.
177. **Takagi, M.; Kawai, T.; Soma, M.; Onishi, T.; Tamaru, K.,** *J. Catal.,* 1977, *50*, 441.
178. **Odrizola, J. A.; Heinemann, H.; Somarjai, G. A.; Garcia de la Banda, J. F.; Pereira, P.,** *J. Catal.,* 1989, *119*, 71.
179. **Inomata, M.; Miyamoto, A.; Murakami, Y.,** *J. Catal.,* 1980, *62*, 140.
180. **Gasior, M.; Haber, J.; Machej, T.; Czeppe, T.,** *J. Mol. Catal.,* 1988, *43*, 359.
181. **Ramis, G.; Busca, G.; Lorenzelli, V.; Forzatti, P.,** *Appl. Catal.,* 1990, *64*, 243.
182. **Dumesic, J. A.; Topsoe, N.-Y.; Slabiak, T.; Morsing, P.; Clausen, B. S.; Tornqvist, E.,** *Proc. 10th Inter. Congr. Catal.,* Elsevier, Budapest, Vol. B, 1992, 1324.
183. **Svachula, J.; Ferlazzo, N.; Forzatti, P.; Tronconi, E.; Bregani, F.,** *Ind. Eng. Chem. Res.,* 1993, *32*, 1053.
184. **Robinson, W. R. A. M.; van Ommen, J. G.; Woldhuis, A.; Ross, J. R. H.,** *Proc. 10th Inter. Congr. Catal.,* Elsevier, Budapest, Vol. C, 1992, 2673.
185. **Spencer, N. D.; Pereira, C. J.,** *J. Catal.,* 1989, *116*, 399.
186. **Pitchai, R.; Klier, K.,** *Catal. Rev. Sci. Eng.,* 1986, *28*, 13.
187. **Liu, H.-F.; Liu, R.-S.; Liew, K. Y.; Johnson, R. E.; Lunsford, J. H.,** *J. Am. Chem. Soc.,* 1984, *106*, 4117.
188. **Sun, Q.; Jehng, J-M.; Hu, H.; Herman, R. G.; Wachs, I. E.; Klier, K.,** (in press).
189. **Mori, K.; Miyamoto, A.; Murakami, Y.,** *J. Chem. Soc., Faraday Trans. 1,* 1986, *82*, 13.
190. **Mori, K.; Miyamoto, A.; Murakami, Y.,** *J. Catal.,* 1985, *95*, 482.
191. **Mori, K.; Inomata, M.; Miyamoto, A.; Murakami, Y.,** *J. Chem. Soc., Faraday Trans. 1,* 1984, *80*, 2655.
192. **Saleh, R.; Wachs, I. E.,** *Appl. Catal.,* 1987, *31*, 87.
193. **Chen, J. C.; Yang, R. T.,** *J. Catal.,* 1990, *125*, 411.
194. **Ramis, G.; Busca, G.; Bregani, F.,** *Catal. Lett.,* 1993, *18*, 299.